Role of electronic excited N_2 in vibrational excitation of the N_2 ground state at high latitudes

L. Campbell,[1] D. C. Cartwright,[2] M. J. Brunger,[1] and P. J. O. Teubner[1]

Received 28 June 2005; revised 12 June 2006; accepted 10 July 2006; published 29 September 2006.

[1] Vibrationally excited N_2 is important in determining the ionospheric electron density and has also been proposed to play a role in the production of NO in disturbed atmospheres. We report here predictions of the absolute vibrational distributions in the ground electronic state of N_2 produced by electron impact excitation, at noon and midnight under quiet geomagnetic conditions and disturbed conditions corresponding to the aurora IBCII$^+$ and IBCIII$^+$ at 60°N latitude and 0° longitude, at altitudes between 130 and 350 km. These predictions were obtained from a model which includes thermal excitation and direct electron impact excitation of the vibrational levels of the N_2 ground state and its excited electronic states; radiative cascade from all excited electronic states to all vibrational levels of the ground electronic state; quenching by O, O_2, and N_2; molecular and ambipolar diffusion; and the dominant chemical reactions. Results from this study show that for both aurora and daytime electron environments: (1) cascade from the higher electronic states of N_2 determines the population of the higher vibrational levels in the N_2 ground state and (2) the effective ground state vibrational temperature for levels greater than 4 in N_2 is predicted to be in the range 4000–13000 K for altitudes greater than 200 km. Correspondingly, the associated enhancement factor for the O^+ reaction with vibrationally excited N_2 to produce NO^+ is predicted to increase with increasing altitude (up to a maximum at a height which increases with auroral strength) for both aurora and daytime environments and to increase with increasing auroral strength. The contribution of the cascade from the excited electronic states was evaluated and found to be relatively minor compared to the direct excitation process.

Citation: Campbell, L., D. C. Cartwright, M. J. Brunger, and P. J. O. Teubner (2006), Role of electronic excited N_2 in vibrational excitation of the N_2 ground state at high latitudes, *J. Geophys. Res.*, *111*, A09317, doi:10.1029/2005JA011292.

1. Introduction

[2] There has been considerable research in the past 30 years on both the production and loss of vibrationally excited N_2 in the thermosphere and its role in ionospheric processes. Excitation and deexcitation of ground state levels of N_2 can occur through thermal processes, direct electron impact, cascade from excited states and chemical reactions. The elevated vibrational temperature increases the contribution of N_2 to ionospheric processes, including reduction of the electron density, formation of high-latitude electron density troughs and NO production.

[3] The N_2 vibrational temperature cannot be measured directly in the thermosphere but at least four attempts have been made, with conflicting conclusions, to extract a temperature value by analysis of various thermospheric data. *Kummler and Bortner* [1972] concluded, based on calculations using models based on species diffusion and measured positive ion concentrations, that the N_2 vibrational temperature is elevated above the kinetic temperature for the lower thermosphere under quiescent conditions. Although they did not include electron impact excitation of N_2, Kummler and Bortner summarized the major mechanisms for producing vibrational excitation in N_2. In a well conceived experiment, *O'Neil et al.* [1974] launched a rocket into an IBC Class II aurora for the purpose of measuring the vibrational population distribution of the $N_2[X^1\Sigma_g^+]$ state in the altitude range 100–200 km (see *Vallance Jones* [1974] for a definition of the IBC auroral index and its relationship to other magnetic disturbance indices). Relative intensities of selected First Negative bands originating from vibrational levels 0, 1, and 2 of the upper electronic state of N_2^+ were combined with a model for the direct electron impact excitation process from ground state N_2 to infer the initial vibrational population of the N_2 ground electronic state. O'Neil et al. concluded that the relative population of $N_2[X(\nu'' = 1)]$ "was not recognizably greater than that based on model atmospheric temperatures" but that the relative population of $N_2[X(\nu'' = 2)]$ was anomalously large. Eleven years later, *Vlaskov and Henriksen* [1985] reported results (from an analysis of ground based emission data from day and night side aurora) based on the same excitation model for N_2^+ as used by *O'Neil et al.* [1974] and

[1] ARC Centre for Antimatter-Matter Studies, School of Chemistry, Physics and Earth Sciences, Flinders University, Adelaide, Australia.
[2] Theoretical Divisions, Los Alamos National Laboratory, Los Alamos, New Mexico, USA.

Copyright 2006 by the American Geophysical Union.
0148-0227/06/2005JA011292

relative intensities of the N_2^+ 1st negative band system. The height of the dayside aurora was assumed to be 150 km and that for the night side aurora 350 km. From their data, they concluded that the effective vibrational temperature on the night side was 500 K greater, and that on the dayside 1000 K greater, than the local kinetic temperature. Most recently, *Kawashima et al.* [1997] reported preliminary results on the inferred N_2 vibrational temperatures obtained by a sounding rocket into the lower thermosphere (100–160 km) under mildly disturbed conditions (F10.7 = 68, Kp = 4). They inferred a vibrational temperature which agreed with the results inferred by *O'Neil et al.* [1974] and was consistent with the analysis of ion data used by *Kummler and Bortner* [1972].

[4] From a historical perspective, *Walker* [1968] and *Walker et al.* [1969] appear to be among the first to report a detailed examination of the production and loss of vibrationally excited N_2 in the normal thermosphere. Walker et al. established that because of its long lifetime, the major loss processes of vibrationally excited N_2 (N_2^*) are downward diffusion above 260 km, stepwise single quantum relaxation by VV (vibration-to-vibration) exchange below 260 km, and energy transfer to CO_2 below 125 km. In their model, *Walker et al.* [1969] did not consider production of N_2^* by thermal electrons or loss by O atom deactivation (both of which were subsequently shown to be important) and estimated the peak N_2 vibrational temperature to be between 1800 and 3600 K at 300 km.

[5] *Schunk and Hays* [1971] assumed production of vibrational quanta by only nonthermal electron sources (i.e., photo and auroral electrons), neglected diffusion, assumed a harmonic N_2 molecule, and examined the time dependence of both the vibrational excitation and O^+ charge exchange processes. They determined that the N_2^* distribution is non-Boltzmann with the lower levels underpopulated and the upper levels overpopulated. They also predicted that at altitudes greater than 200 km, the O^+ charge exchange rate with N_2^* is 50% greater than that for a Boltzmann vibrational distribution.

[6] *Varnum* [1972] extended the work by *Walker et al.* [1969] and *Kummler and Bortner* [1972] on the production of N_2^* in the normal thermosphere under solar minimum conditions, by expanding the model to include excitation and deexcitation by thermal electrons and also examined N_2^* formation under solar maximum conditions. Varnum's results confirmed the findings of both *Walker et al.* [1969] and *Kummler and Bortner* [1972] that at 300 km, the maximum temperature for low solar activity is about 1800 K and that for high solar activity about 3000 K. This work by Varnum, and an independent (but simultaneous) one by *Vlasov* [1972], appear to have been the first to establish the importance of thermal electrons in determining the vibrational population of N_2.

[7] In a definitive work on the role of vibrationally excited N_2 in stable auroral red (SAR) arcs, *Newton et al.* [1974] reported (1) that the N_2^* vibrational distribution deviated substantially from a Boltzmann distribution and (2) that O^+ charge exchange with N_2^* is enhanced by a factor of 7.6 at F2 region altitudes. Newton et al. solved the continuity equation for the first six vibrational levels of N_2, assuming production of N_2^* by thermal electrons, collisions with O atoms, VV exchange between N_2 molecules, and transitions only between neighboring vibrational levels (i.e., that the harmonic oscillator approximation is valid for N_2). Newton et al. appear to have been the first to include the (then recently discovered [*Breig et al.*, 1973]) quenching of N_2^* by O atoms as the major loss process for altitudes in the 120–300 km range, in addition to those loss processes reported by *Walker et al.* [1969]. They were frequently cited in subsequent papers because they included (in an appendix) a tabulation of the production and loss rates for the first six vibrational levels of N_2, as a function of the electron temperature. Walker et al. also confirmed the result of *Varnum* [1972] as to the importance of thermal electrons in producing N_2^* and the earlier prediction that the density of vibrationally excited N_2 increases with altitude.

[8] In 1978 and 1979, two independent modeling studies [*Vlasov et al.*, 1978; *Waite et al.*, 1979] were performed which led the respective authors to conclude that the N_2 vibrational distributions formed in both the midlatitude and high-latitude disturbed (IBC Class II and III aurora) *E* region were Boltzmann at the local temperature rather than significantly enhanced. This conclusion, which contradicted earlier conclusions for the same environments, appears to have been based on excitation models which are too simplified to adequately model the excitation process. In a subsequent study, *Vlasov and Izakova* [1980] reported that an enhanced N_2 vibrational distribution was responsible for the seasonal behavior in the peak of the *F* region electron density. They predicted a decrease in electron density in the *F* peak by a factor of 2 due to an increase in the rate coefficient of the reaction of O^+ with N_2^* in summer at middle latitudes, which explained the winter anomaly.

[9] Beginning in the late 1970s, the availability of year-round satellite data on the particle composition of the ionosphere motivated researchers to use more comprehensive computer models to determine if N_2 is indeed vibrationally excited at some altitudes under certain conditions. Guided by satellite data, *Torr et al.* [1980] concluded that one of the three causes for the *F* region "winter anomaly" was the enhanced charge exchange reaction of O^+ due to the presence of vibrationally excited N_2. *Richards et al.* [1986] and *Richards and Torr* [1986] showed that under certain circumstances, N_2^* could play a central role in determining both the temperature and density of ionospheric electrons. *Richards et al.* [1986] showed that depending on the values chosen for the relative magnitudes of the N_2^* and O atom cooling rates, cooling of thermal electrons by N_2^* may be the dominant cooling mechanism. In addition, *Richards et al.* [1986] appear to be the first to identify that electron impact excitation of N_2 triplet electronic states, eventually resulting in radiative cascade from the A state into vibrational levels of the N_2 ground state, could be a major source of N_2 vibrational quanta in the normal ionosphere and could be the dominant mechanism for producing vibrationally excited N_2 in the aurora.

[10] *Richards and Torr* [1986] showed that enhancement of the O^+ charge exchange by N_2^* in summer at solar maximum could be sufficient to reduce the O^+ density by a factor of two. They also defined a useful parameter called the "enhancement factor", used later in this work, to characterize the overall charge exchange reaction of O^+ with vibrationally excited N_2 relative to that for N_2 in the lowest vibrational level. Results from these earlier studies

will be compared, in detail, with those from the present work in section 4.2.

[11] *Rodger et al.* [1992] reviewed the progress that had been made in describing the phenology and morphology of midlatitude troughs (i.e., reduced electron density) and provided a summary of the characteristics associated with high-latitude troughs. They reported that midlatitude troughs are usually a feature of the night side ionosphere and that high-latitude troughs, occurring within the auroral oval, are associated with regions of electron precipitation and relatively strong electric fields. In addition, there is usually a higher-than-normal concentration of NO^+ in troughs where the E field is strong and, in some cases, the electron and ion temperatures are greater than normal. Rodger et al. identified the need to characterize those regions and conditions where vibrationally excited N_2 (N_2^*) and O_2 (O_2^*) are formed in the ionosphere and clarify their relative roles in trough formation.

[12] During the past 10 years, a number of authors have made significant contributions to the understanding of the production and loss of vibrationally excited nitrogen (N_2^*) in the thermosphere as well as the role this metastable species might play in determining thermospheric properties through the use of increasingly sophisticated computer models. A brief summary of the models used and results obtained, from the published literature, is given here for completeness.

[13] In a series of papers, Ennis, Bailey, Moffett and coworkers have used the Sheffield University plasmasphere ionosphere model (SUPIM) to examine the dependence of N_2^* on the season and solar cycle [*Ennis et al.*, 1995]; the effect of N_2^* on the low-latitude ionosphere [*Jenkins et al.*, 1997]; and subauroral ion drift (SAID) events [*Moffett et al.*, 1998]. *Ennis et al.* [1995] assumed a Boltzmann distribution of quanta, neglected photoelectron excitation, assumed that the high-energy tail of the thermal electron distribution was the major source of vibrational excitation of N_2 (i.e., no cascade from higher electronic states or excitation by photoelectrons), included only the lowest six vibrational levels of N_2, and assumed that quenching by O atoms and charge exchange with O^+ were the only loss processes for N_2^*. Their results confirmed the earlier findings of *Richards and Torr* [1986] that vibrationally excited N_2 is important at solar maximum. More specifically, *Ennis et al.* [1995] found that at 300 km in the summer at high solar activity, ~9% of N_2 is in $\nu'' = 1$ and ~5% in $\nu'' > 1$, and for low solar activity, 80% or less of all the vibrationally excited N_2 molecules are in $\nu'' = 1$. In their model, production of N_2^* is driven by the electron temperature and there is a positive feedback mechanism between the local electron temperature and the excited vibrational population.

[14] *Jenkins et al.* [1997] extended the model used in the *Ennis et al.* [1995] study to investigate the effects of vibrationally excited N_2 on the low-latitude ionosphere. They found that the production of N_2^* increases with increasing electron density and electron temperature and, in contrast to the situation at midlatitudes, N_2^* significantly reduces the electron density in all seasons. They concluded that N_2^* can have a significant effect on the low-latitude ionosphere and, if present in the equatorial trough, N_2^* could cause reduction of the electron density to two thirds of its value without N_2^* present.

[15] In another application of the SUPIM model, *Moffett et al.* [1998] examined the parameters which could affect the electron temperatures during rapid SAID events. As was the case in the two previous studies, Moffett et al. found that N_2^* plays a role in determining both the electron density and temperature of the trough within a SAID event because of enhanced charge exchange with O^+.

[16] In two detailed papers, *Vlasov and Smirnova* [1995a, 1995b] examined the effect of vibrational anharmonicity in the N_2 ground state on both the vibrational kinetics and the O^+ charge exchange with N_2^*. In their first paper on the vibrational distribution established in N_2 in the thermosphere for conditions of low and high solar activity, *Vlasov and Smirnova* [1995a] predicted distributions which deviated substantially from a Boltzmann distribution. Specifically, they found that for fixed solar activity the deviation (1) decreased with increasing altitude and (2) at fixed altitude, the deviation decreased with increasing solar activity. *Vlasov and Smirnova* [1995b] found that incorporation of anharmonicity in the N_2 ground state resulted in a significant increase in the rate constant for O^+ charge exchange with N_2^*. Results from these earlier studies will also be compared with those from the present work in section 5.2.

[17] Pavlov and coworkers have been prolific contributors to the knowledge base on both the production of N_2^* and the effect of this species on the structure and dynamics of the ionosphere [*Pavlov and Namgaladze*, 1988; *Pavlov*, 1993; *Pavlov and Buonsanto*, 1996; *Pavlov*, 1998a, 1998b; *Pavlov and Oyama*, 2000; *Pavlov et al.*, 2000]. However, it appears that the model used by Pavlov and coworkers treated only direct excitation and neglected the effects of radiative cascade from higher N_2 electronic states. Nonetheless, because of the recognized importance of direct electron excitation in the production of vibrationally excited N_2, *Pavlov* [1998b] reported a thorough and useful reevaluation of the relevant excitation cross sections since the work reported by *Stubbe and Varnum* [1972] and by *Newton et al.* [1974] and also provided tables of coefficients for the temperature dependence of the Maxwell-averaged excitation rates based on updated cross sections. The excitation cross sections used in this study have been revised since the work on this subject by *Pavlov* [1998b] and are from the recommended new set of excitation cross sections reported by *Campbell et al.* [2004].

[18] *Vlasov and Kelley* [2003] have reported results from a model to explain the formation of high-latitude electron density troughs under the conditions of strong magnetic activity and low average-energy precipitating electrons. The essence of their model is that vibrationally excited N_2 is produced poleward of the observed density trough (at altitudes above 150 km) and, because of the relatively long lifetime for N_2^* and southward convection, N_2^* is transported to the south where there is no electron precipitation. The resulting enhanced charge exchange reaction with O^+ to form NO^+, the fact there is no local electron precipitation to maintain ion formation, and the rapid recombination of NO^+, results in the observed electron density trough. Results from their model appear to better explain the time dependence of trough formation observed on 20 April 1985

than previous models. In applying their model, Vlasov and Kelley used the enhanced reaction rate coefficients for the O^+ charge exchange reaction from *Vlasov and Smirnova* [1995b, 1997] and a model for the vibrational kinetics from *Vlasov and Smirnova* [1995a]. We will compare our predictions with certain of the results predicted by the Vlasov and Smirnova models in section 5.2.

[19] In addition to its known effect on the electron density, vibrationally excited N_2 has also been postulated to enhance the formation of NO, in the disturbed polar thermosphere, as a result of the exothermic chemical reaction of O atoms with vibrational levels >11 in the ground electronic state of molecular nitrogen [*Gordiyets*, 1977; *Rusanov et al.*, 1981], and with the metastable $A^3\Sigma_u^+$ state [*Swider*, 1976; *Reidy et al.*, 1982]. In pursuit of this concept, a variety of field-induced and plasma interactions have been evaluated as mechanisms to increase the effective vibrational temperature of N_2 in the polar thermosphere and, thereby, produce the observed enhanced NO density in the disturbed thermosphere [*Vlasov et al.*, 1980; *Zhdanok and Telegin*, 1983; *Mishin and Telegin*, 1989]. These postulated mechanisms of NO formation are included in our model, and their contribution to the NO density will be specifically considered in a companion paper to the present study (L. Campbell et al., The role of excited N_2 in the production of nitric oxide, manuscript in preparation, 2006).

[20] Although a number of different excitation and environment models have been evaluated for producing an enchanced N_2 vibrational population (see, e.g., *Pavlov and Buonsanto* [1996] for a review of these models), it appears that no analysis of the electron impact produced vibrational distribution of N_2 has been reported which treats self-consistently both the excited electronic states and the vibrational levels of the N_2 ground state. More specifically, except for the work by *Richards et al.* [1986], previous researchers on this topic have used models in which the N_2 vibrational population is produced only by thermal excitation and/or direct electron impact from the $N_2[X(\nu'' = 0)]$ initial state to higher ν'' levels. This paper reports results from an expanded excitation model for N_2 in which the excited electronic vibrational states and vibrational levels of the ground state are treated self-consistently. More specifically, this paper reports an analysis of the thermal and electron impact production of vibrationally excited N_2, at altitudes between 130 and 450 km, for undisturbed day and night conditions, and for aurora of intensity IBC Class II^+ and III^+ (where it is assumed that the "+" superscript denotes 4 times the intensity for the same class aurora with no superscript).

[21] The goal of this work is to predict the absolute vibrational distributions in the ground electronic state of N_2 produced by electron impact excitation, at noon and midnight under quiet geomagnetic conditions and disturbed conditions corresponding to the aurora IBC II^+ and IBC III^+ at 60° N latitude and 0° longitude, at altitudes between 130 and 350 km. A subsidiary goal is to examine the associated enhancement factor for the O^+ reaction with vibrationally excited N_2 to produce NO^+ for both aurora and daytime environments, with increasing auroral strength.

[22] In section 2 we review the mechanisms for production and loss of vibrationally excited N_2. Section 3 presents the details of the method of calculation and the model of electron flux spectra used for this study. In section 4, calculated results of the model are presented, including production rates, populations and temperatures of vibrationally excited nitrogen. Some comparisons are made with previous work. In section 5 the vibrational distributions predicted by our expanded model are then used to estimate the associated enhancement of the O^+ charge transfer reaction rate.

2. Mechanisms for Production and Loss of Vibrationally Excited N_2

2.1. Direct Electron Impact Excitation

[23] The first measurements of the cross sections for electron impact vibrational excitation of N_2 were made by *Schulz* [1964, 1976]. All experimental and theoretical data for direct electron impact excitation of vibrational quanta in the ground electronic state of $N_2[X^1\Sigma_g^+]$ reported since the work by *Trajmar et al.* [1983] were recently reviewed by *Brunger and Buckman* [2002]. On the basis of this review, *Campbell et al.* [2004] recommended an improved set of integral cross sections for describing direct electron impact excitation of the vibrational levels in $N_2[X(\nu'' = 0)]$. Campbell et al. also reported electron energy transfer rates for this recommended set of cross sections for a Maxwellian distribution of electrons characterized by a range of electron temperatures appropriate for the Earth's thermosphere. The direct excitation cross sections suggested by *Campbell et al.* [2004] were used in this study to treat direct electron impact excitation of the vibrational levels from $N_2[X(\nu'' = 0)]$ (The energy transfer rates were not used here as they are specific to a thermal electron distribution and not appropriate for the non-Maxwellian distributions of photo and auroral electrons. Rather the full calculation of the integrated product of cross section and flux as a function of energy is used.).

2.2. Cascade From the Higher Electronic States of N_2

[24] In their modeling of the ionospheric electron density, *Richards et al.* [1986] recognized the potential importance of cascade from the $N_2[A^3\Sigma_u^+]$ electronic state in determining the vibrational population of the higher vibrational levels of the $N_2[X]$ state. Although Richards et al. concluded that a quantitative study of the A–X cascade effect was outside the scope of their investigation, they did estimate the magnitude of the A–X cascade and concluded that it could be important. To our knowledge, no results have been reported from a quantitative assessment of the effect of radiative cascade in determining the vibrational population of the N_2 ground state. This work, which self-consistently treats thermal, direct, and cascade contributions to the $N_2[X]$ state vibrational distribution is an attempt to remove that deficiency, as follows.

[25] Radiative cascade contributions to the $N_2[X]$ state vibrational distribution from higher electronic states can now be calculated reasonably accurately using the equations of statistical equilibrium for N_2 in an electron environment. The statistical equilibrium model has been used for predicting and interpreting auroral [*Cartwright*, 1978; *Morrill and Benesch*, 1996; *Cartwright et al.*, 2000] and dayglow [*Broadfoot et al.*, 1997; *Morrill et al.*, 1998; *Eastes*, 2000] excitation of atoms and molecules. The statistical equilibrium

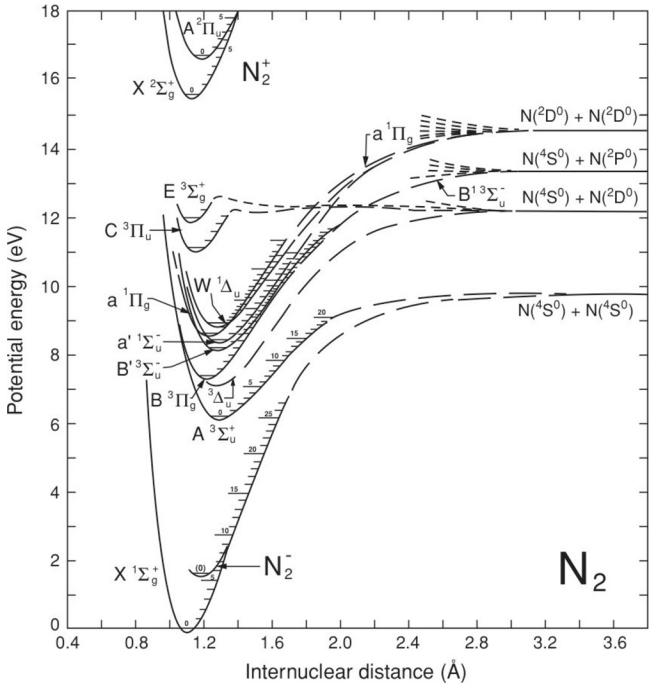

Figure 1. A simplified version of the potential energy curves for N_2, as a function of the internuclear distance, taken from *Gilmore* [1965]. Note the larger internuclear separations of the valence excited states relative to that for the ground state. The E and C excited states above 11 eV are typical Rydberg states (see main text).

model works well for determining populations in the excited electronic states of N_2 because these states are not directly populated by VV and VT transitions or chemical reactions.

[26] As will be shown quantitatively, radiative cascade from higher electronic states is the mechanism which determines the vibrational population in the middle and high vibrational levels of the $N_2[X]$ state (i.e., $\nu'' > 4$). This important property can be understood qualitatively by noting that all N_2 excited electronic states which radiate, except the energetically high-lying Rydberg state $c'^1\Sigma_u^+$, have equilibrium internuclear separations which are larger than that for the $N_2[X]$ state. This means that radiative cascade (or quenching) into the X state from excited N_2 electronic states generally favors population of vibrational levels greater than 1 in the X state (see *Lofthus and Krupenie* [1977, Table 83, pp. 256, 262] for Franck Condon arrays for the A–X and a–X transitions). This general characteristic of the N_2 excited electronic states can also be recognized from the shapes, and relative locations of the minima, of the potential energy curves shown in Figure 1. The reason that radiative cascade is important in determining the vibrational population of the X state, as recognized by *Richards et al.* [1986], is that all the energy deposited in the triplet excited vibronic (i.e., vibrational electronic) states in N_2 eventually collects in the vibrational levels of the $A^3\Sigma_u^+$ state. Hence, when the $A^3\Sigma_u^+$ state radiates (producing the Vegard-Kaplan bands), it preferentially populates the higher vibrational levels of the X state because the average internuclear separation in the A state is substantially larger than that in the ground state (see Figure 1).

[27] A potential exception to this characteristic of the excited states of N_2 are the high-lying singlet states which are not shown in Figure 1 but are similar in energy and shape to the C and E states given in Figure 1. These excited Rydberg states have internuclear separations close to that for the X state and would populate the lowest vibrational levels of the X state if they radiatively decay. However, on the basis of an experimental study, *Cosby* [1993] showed that all the high-lying singlet Rydberg states of N_2 except the $c'^1\Sigma_u^+$ state dissociate into atomic fragments before they radiate. As a consequence of these results from *Cosby* [1993], we believe that the valence singlet and triplet excited states plus the $c'^1\Sigma_u^+$ Rydberg state account for all the electronic states of N_2 which populate the vibrational levels of the X state by radiative cascade. Thus these were the excited electronic states used in this study of the cascade contribution to the population of the vibrational levels of N_2 in the thermosphere.

2.3. Collisional Mechanisms

[28] The effect of chemical reaction and energy transfer mechanisms [e.g., energy transfer from $O(^1D)$] has been modeled extensively [e.g., *Walker et al.*, 1969; *Vlasov*, 1972; *Newton et al.*, 1974; *Richards et al.*, 1986; *Richards and Torr*, 1986; *Pavlov*, 1993; *Vlasov and Smirnova*, 1995a]. This study includes the production of N_2^* by the reaction between $N(^4S)$ atoms and NO, the loss due to the reaction of O atoms with N_2^* to form NO, and the redistribution between N_2^* levels due to VT and VV transitions and collisions with O atoms, as detailed below.

2.4. Molecular Diffusion

[29] Because of the relatively long lifetime of N_2^*, it is necessary to account for molecular diffusion, which causes a net movement of N_2^* downward. This is implemented by application of the equations given by *Kolesnik* [1982], but using the diffusion coefficient specified by *Jenkins et al.* [1997].

3. Details of the Model Used in This Study

3.1. Main Processes and Method of Calculation

[30] Many physical and chemical processes involving the N_2 molecule in its ground and excited states have been thoroughly studied. For example, the electron impact excitation cross sections [*Campbell et al.*, 2001; *Brunger and Buckman*, 2002], radiative transition probabilities [*Gilmore et al.*, 1992], and quenching rates [e.g., *Herron*, 1999; *Strickland et al.*, 1999] are now all relatively well known (that is, compared to O_2 and NO). Therefore, once the details of the electron environment (i.e., the local electron energy distribution) are specified, the equations for statistical equilibrium can be solved to predict the N_2 ground state vibrational distribution produced directly or indirectly (i.e., cascade) by electron impact excitation. However, a self-consistent treatment of all electron impact processes in N_2 which affect the excited N_2 vibrational levels requires that excitation and deexcitation from the excited vibrational levels (i.e., $\nu'' > 0$) also be included as well as excitation from the lowest vibrational level (i.e., $\nu'' = 0$) of the X state. The cross sections for excited-to-excited transitions between the vibrational levels of ground state N_2, required for a self-

Table 1. Reactions Used Which Differ From the Model of *Barth* [1992]

Reaction	Rate, cm^3 $molecule^{-1}$ s^{-1}, or Description	Source
$N_2 + e_s^- \rightarrow N_2^* + e_s^-$	full cross section used	*Brunger et al.* [2003]
$N_2^* \rightarrow N_2 + h\nu$	individual levels	*Gilmore et al.* [1992]
$N_2^* + N_2, O_2, O, NO \rightarrow N_2 + N_2 \ldots$	individual levels	*Cartwright* [1978]
$N_2(\nu'') + O \rightarrow N_2(\nu'' - 1) + O$	$1.07 \times 10^{-10}\exp(-69.9/T_n^{1/3})$	*Pavlov and Buonsanto* [1996]
$NO + N(^4S) \rightarrow N_2(\nu'' = 4)] + O$	4.0×10^{-11}	*Jenkins et al.* [1997]
$O_2 + e_s^- \rightarrow O_2^+ + 2\ e_s^-$	full cross section used	*Lindsay and Mangan* [2003]
$O + e_s^- \rightarrow O^+ + 2\ e_s^-$	full cross section used	*Itikawa and Ichimura* [1990]
$N_2 + e_s^- \rightarrow N_2^+ + 2\ e_s^-$	full cross section used	D. C. Cartwright (private communication, 2001)
$N_2 + e_s^- \rightarrow N(^4S) + N(^2D) + e_s^-$	full cross section used	*Cosby* [1993]
$N_2[X^1\Sigma_g^+(\nu'' > 11)] + O \rightarrow NO + N$	10^{-11}	*Aladjev and Kirillov* [1995]
$N_2[A^3\Sigma_u^+] + O \rightarrow NO + N(^2D)$	2×10^{-11}	*Kochetov et al.* [1987]
$N_2[A^3\Sigma_u^+] + O \rightarrow O(^1S) + N_2$	$2.5 \times 10^{-11}(T_n/298)^{0.55}$	*Herron* [1999]
$N(^2D) + O_2 \rightarrow NO^* + O$	$9.7 \times 10^{-12}\exp(-185/T_n)$	*Herron* [1999]
$N(^4S) + O_2 \rightarrow NO + O$	$1.15 \times 10^{-11}\exp(-3503/T_n)$	*Swaminathan et al.* [1998]
$NO + N(^2D) \rightarrow N_2 + O$	6×10^{-11}	*Herron* [1999]
$N(^2D) + O \rightarrow N(^4S) + O$	$1.4 \times 10^{-12}\exp(-259/T_n)/\exp(-259/298)$	*Herron* [1999]
$N(^2D) \rightarrow N(^4S) + h\nu$	transition probability 2.3×10^{-5} s^{-1}	*Wiese et al.* [1996]
$O^+(^4S) + O_2 \rightarrow O_2^+ + O$	$1.6 \times 10^{-11}\exp(300/T_n)^{0.52} + 5.5 \times 10^{-11}\exp(-6835/T_n)$	*Pavlov* [1998a]
$O^+(^2P) \rightarrow O^+(^2D) + hv$	0.171 s^{-1}	*Torr et al.* [1979]
$O^+(^2D) + O \rightarrow O^+(^4S) + O$	10^{-10}	*Pavlov and Buonsanto* [1998]
$O^+(^2P) + N_2 \rightarrow N_2^+ + O$	4.8×10^{-10}	*Torr et al.* [1979]
$O^+(^2P) + O \rightarrow O^+(^4S) + O$	5.2×10^{-11}	*Torr et al.* [1979]
$O^+(^2P) \rightarrow O^+(^4S) + hv$	0.047 s^{-1}	*Torr et al.* [1979]

consistent analysis, are known only approximately. These transitions were included in the equations solved in this study by incorporating the recent cross sections reported by *Campbell et al.* [2004]. The basic statistical equilibrium model used in this study is similar to that reported earlier [*Cartwright*, 1978; *Cartwright et al.*, 2000] except for the following:

[31] 1. The 21 vibrational levels for the N_2 ground electronic state were included in the set of equations compared to the earlier study which used only the lowest level.

[32] 2. Some chemical reactions involving excited nitrogen have been added:

$$N_2\left[X^1\Sigma_g^+(\nu'' > 11)\right] + O \rightarrow NO + N \text{ [Rusanov et al., 1981]}$$

$$N_2\left[A^3\Sigma_u^+\right] + O \rightarrow NO + N(^2D) \text{ [Herron, 1999]}$$

$$N + NO \rightarrow N_2\left[X^1\Sigma_g^+(\nu'' = 4)\right] + O \text{ [Jenkins et al., 1997]}$$

$$O + N_2\left[X^1\Sigma_g^+(\nu'')\right] \rightarrow N_2\left[X^1\Sigma_g^+(\nu'' - 1)\right] + O \text{ [Pavlov and Namgaladze, 1988]}$$

[33] 3. VV and VT transitions (using equations by *Kirillov* [1998]) have been included.

[34] 4. Photoionization, using the model of *Richards et al.* [1994], with the flux at the shortest wavelengths increased as suggested by *Solomon et al.* [2001]. The most significant consequent chemical and recombination reactions (as listed in the model of *Barth* [1992] and the AURIC model [*Strickland et al.*, 1999]) were included, allowing a calculation of the electron density. Table 1 lists those reactions included in this study which were additional to those listed by Barth and Strickland et al., or for which different rates have been used.

[35] 5. Ambipolar diffusion of O^+ was implemented using equations given by *Buonsanto et al.* [1997]. Diffusion of $N(^4S)$ atoms was included using the diffusion coefficient specified by *Bailey et al.* [1997].

[36] If it is assumed that excitation occurs only from the lowest vibrational level ($\nu'' = 0$) of the N_2 ground electronic state, the equations for statistical equilibrium for each vibrational level (ν') of electronic state (α) are [*Cartwright et al.*, 2000]

$$\left(1 - Q'^{\alpha}_{\nu'}\right)\left(k^{\alpha}_{\nu' 0} n_0^x + \sum_{\beta}\sum_{i} A^{\beta\alpha}_{i\nu'}\, n_i^{\beta}\right) = \left[\sum_{i,j,k}\left(A^{\alpha j}_{\nu' i} + Q^{\alpha k}_{\nu'}\right) + \sum_{i,j,K}\left(C^{\alpha K}_{\nu'}\right)\right] n^{\alpha}_{\nu'} \quad (1)$$

where

$$k^{\alpha}_{\nu' 0} = \int_0^{\infty} F(E)\, \sigma^{\alpha}_{\nu' 0}(E)\, dE \quad (2)$$

is the electron impact excitation rate of vibrational level ν' in state α, E is the electron energy, $F(E)$ is the altitude-dependent electron distribution (thermal plus the photoelectron or auroral secondary electron spectrum), n_0^x is the number density of N_2 molecules in the ground electronic vibrational state, $n^{\alpha}_{\nu'}$ is the number density of vibrational level ν' in electronic state α, $\sigma^{\alpha}_{\nu' 0}$ (cm^2) is the rotationally averaged electron impact excitation integral cross section for the ν'th vibrational level in electronic state α, $A^{\beta\alpha}_{i\nu'}$ (s^{-1}) is the transition probability connecting vibrational levels i and ν' in electronic states β and α, respectively, $Q^{\alpha k}_{\nu'}$(s^{-1}) is the quenching rate of vibrational level ν' in electronic state

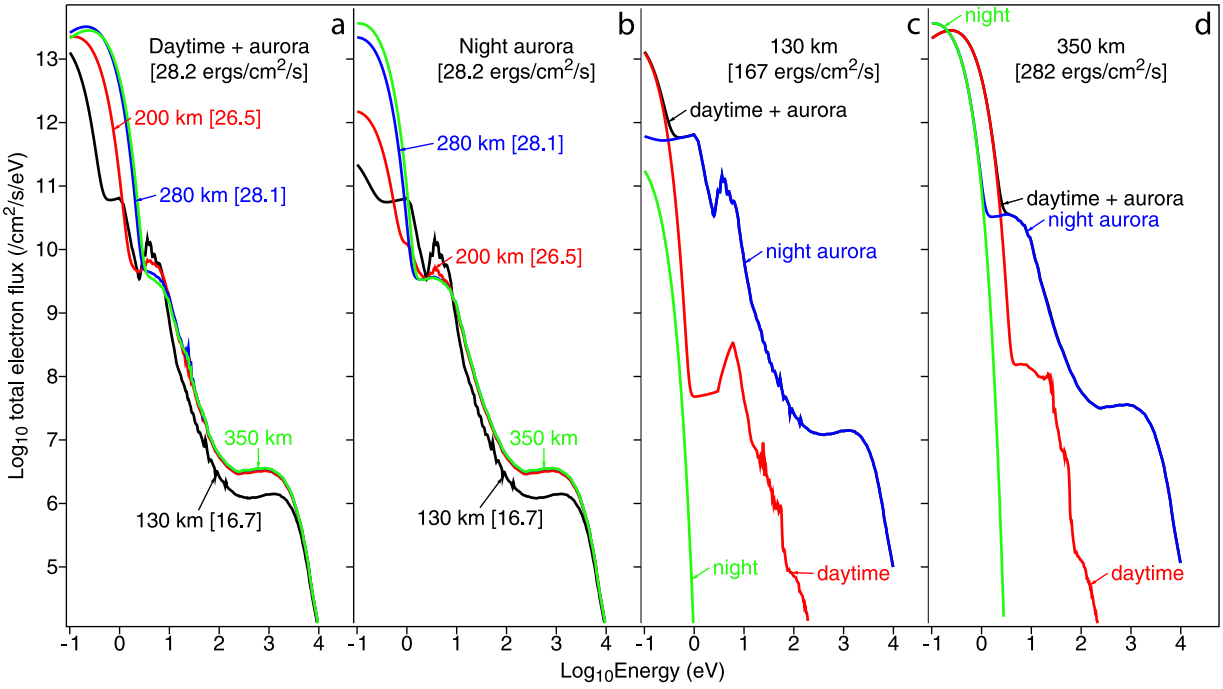

Figure 2. Model electron spectra for 130, 200, 280 and 350 km used in this study for different electron environments. (a) Daytime plus aurora; (b) aurora at night; (c) daytime + aurora, night aurora, daytime, and night thermal, all at 130 km and for an IBC III$^+$ aurora; (d) daytime + aurora, night aurora, daytime, and night thermal, all at 350 km and for an IBC III$^+$ aurora.

α by species k [O_2, N_2, O], $C_{\nu'}^{\alpha K}$ is the loss rate of molecules in vibrational level ν' in electronic state α by chemical reaction K and $Q_{\nu'}^{\prime\alpha}$ is the predissociation probability for the vibrational level ν' in electronic state α.

[37] For the ground state vibrational levels electron impact deexcitation, stepwise quenching, molecular diffusion and thermal transitions are also included

$$\sum_i k_{\nu' i}^x n_i^x + \sum_K C_{\nu'}^{\prime K} + \sum_i A_{i\nu'}^{xx} n_i^x + VT_{(\nu'\pm1)\nu'} n_{\nu'\pm1}^x n_0^x + \sum_i VV_{(\nu'\pm1)\nu'}^{(i\mp1)i} n_{i\mp1}^x n_{\nu'\pm1}^x + Q_{\nu'+1}^S n_{\nu'+1}^x - \frac{\partial F_{\nu'}}{\partial z} = \left[\sum_i A_{\nu' i}^{xx} + \sum_K C_{\nu'}^{xK} + VT_{\nu'(\nu'\pm1)} n_0^x + \sum_i VV_{\nu'(\nu'\pm1)}^{i(i\mp1)} n_i^x + Q_{\nu'}^S\right] \cdot n_{\nu'}^x \quad (3)$$

where $VT_{\nu'(\nu'+1)}$ is the rate of VT transitions from level ν' to $\nu'+1$, $\sum_i VV_{(\nu'+1)\nu'}^{(i-1)i}$ is the rate of the vibrational exchange where a collision between N_2 molecules in levels $\nu'+1$ and $i-1$ leaves them in levels ν' and i, respectively, $C_{\nu'}^{\prime K}$ is the production rate of N_2 in level ν' due to chemical reaction K, $Q_{\nu'}^S$ is the rate of stepwise quenching of level ν' by O atoms and $\partial F_{\nu'}/\partial z$ is the loss rate due to molecular diffusion at altitude z [*Kolesnik*, 1982].

[38] In the statistical equilibrium calculation, the continuity equations for all species were repetitively solved until all computed densities converged to equilibrium values. An obvious question is whether or not equilibrium is actually achieved in the atmosphere. To resolve this, a time step simulation was also performed, in which the change in each species was calculated for a small time interval, with this calculation being repeated over a large number of such intervals. This time step simulation is not practical for the calculation of populations of the excited states of N_2 because the wide range of radiative transition probabilities would require a prohibitively large number of small time intervals. However, time step simulation can be used to predict the populations of the ground state vibrational levels because the radiative transition probabilities are very small (i.e., quadrapole). Hence time step calculations were performed for all processes (ionization, chemical reactions and transitions between ground state vibrational levels) except those between the excited states, for which the populations are imported from the statistical equilibrium calculation.

[39] The equilibrium calculation was run for noon or midnight at longitude 0°, latitude 60° for 21 June 2001, chosen to give atmospheric conditions at solar maximum. For daytime the time step calculation was run with 0.1-s steps for a 6-hour interval ending at noon with the aurora (if included) applied for the last 6 min. At night the initial O^+ and electron densities were set to the value of the electron density at midnight from the International Reference Ionosphere (IRI) empirical model [*Bilitza*, 2001] and a 6-min aurora then applied. Calculations were performed simultaneously at 48 heights at 10-km intervals in the altitude range 130–600 km, to allow molecular diffusion and ambipolar diffusion to be calculated.

[40] The calculation of the gain $-\partial F_{\nu'}/\partial z$ due to molecular diffusion requires a boundary condition at the top and bottom heights. Diffusive equilibrium was assumed at the upper height, by setting the flux $F_{\nu'} = 0$. At the lower height the value was determined by extrapolation from the two heights above the boundary.

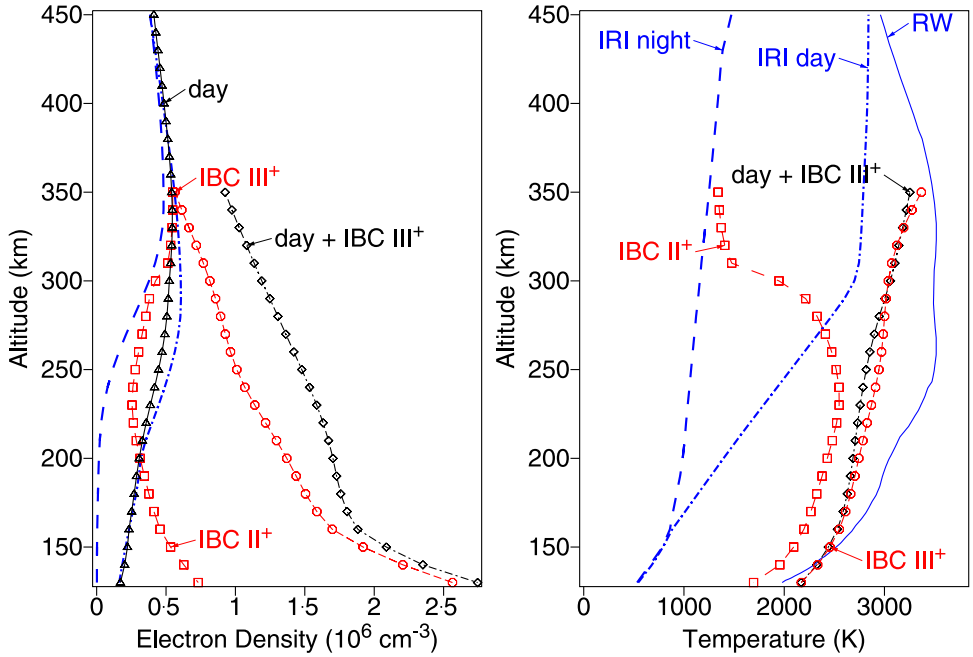

Figure 3. Electron density and temperature, at the end of the time step calculation, as a function for altitude for four different electron environments: (curve with triangles) daytime (density only); (dashed curve with squares) IBC II^+ aurora at night; (dashed curve with open circles) IBC III^+ aurora at night; (dashed curve with diamonds) daytime plus IBC III^+ aurora. The temperatures and densities from the IRI for daytime (dot-dashed curve) and nighttime (dashed curve) and the auroral temperature calculated by Rees and Walker [*Vallance Jones*, 1974] (solid curve) are also shown.

3.2. Electron Energy Distributions for the Normal and Disturbed Thermosphere

[41] In order to obtain realistic predictions for the volume production of vibrationally excited N_2 in the thermosphere produced by electron impact, it is necessary to have realistic descriptions of the altitude distributions for thermal, photoelectron, and auroral electrons. In this study, we used the following electron distributions (see Figure 2 and text below) for these three different environments.

3.2.1. Thermal Electrons

[42] A Maxwellian electron distribution initially characterized by an electron temperature and density from the International Reference Ionosphere [*Bilitza*, 2001; IRI, 2004, http://nssdc.gsfc.nasa.gov/space/model], with the electron density then recalculated as part of the model by assuming that the density is equal to the density of positive ions produced by ionization. The ionization rates are calculated by multiplying the photoelectron and auroral distributions described below by cross sections for the ionization of O, N_2, and O_2. The calculation of the higher electron temperature produced by the aurora is described below.

3.2.2. Photoelectrons

[43] The photoelectron distribution reported by *Strickland et al.* [1999] and D. J. Strickland (private communication, 2002) for medium solar activity at a solar zenith angle of 0°. This was scaled to solar maximum and other zenith angles by the ratio of the photoionization rate for these conditions to the value given by calculating the photoionization rate for the conditions specified by Strickland.

3.2.3. Auroral Electrons

[44] The electron spectra measured by *Feldman and Doering* [1975], approximately constant for the altitude range 120–162 km, and that measured by *Lummerzheim et al.* [1989] for 340 km were used as reference electron spectra for determining the electron spectrum used in this study. These two sets of measurements, although at different altitudes, appear to have been performed for about the same strength aurora because both studies reported a 557.7 nm intensity of 40 kR, corresponding to a medium strength [IBC II^+] aurora. For the spectrum measured by Feldman and Doering, no simultaneous measurement of the primary energy flux was made but it was estimated to vary over the range 1 to 27 ergs cm^{-2} s^{-1}. For the spectrum at 340 km, *Lummerzheim et al.* [1989] measured an energy flux of 27 ergs cm^{-2} s^{-1} with a characteristic energy of 3.1 keV. In our study the shape of the distribution was taken from the model of *Lummerzheim and Lilensten* [1994], with their values scaled (× 27) to roughly match the total energy in the model spectrum to the specific measurements above. Our distributions for 130 km and 350 km were set to those of *Lummerzheim and Lilensten* [1994] at 150 km and 300 km, respectively, both multiplied by a factor of 27. The distribution for 130 km was extended below 1eV using the shape of the low-energy spectrum measured by *Sharp and Hays* [1974]. The assumed secondary electron distributions at other heights were then obtained by interpolation between the values at 130 km and 350 km, using

$$F_h = F_{130} + \frac{E_h - E_{130}}{E_{350} - E_{130}}(\mathrm{F}_{350} - \mathrm{F}_{130}) \quad \text{where } E_{h'} = 1 - e^{-0.027(h'-60)} \tag{4}$$

where F_h is the flux at height h (km). Above 350 km the flux was determined by a logarithmic fit to the spectrum at

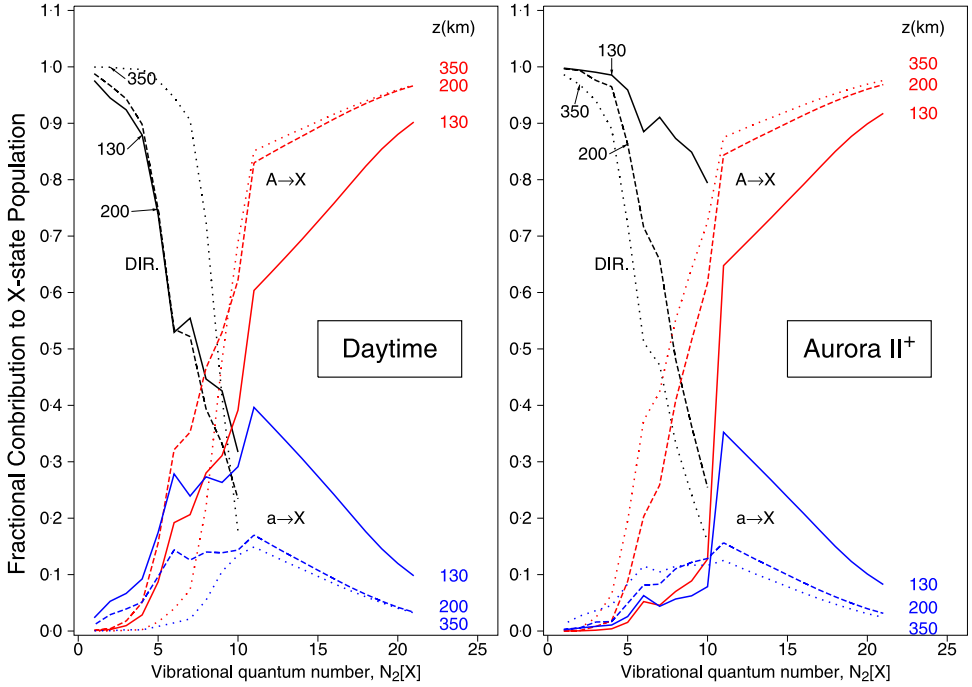

Figure 4. Fractional contributions, by direct excitation and by radiative cascade from the A and a states, (left) to the total vibrational population of N_2 under daytime and (right) IBC II^+ auroral environments, for altitudes of 130, 200, and 350 km.

350 km and 27× the calculated spectrum at 500 km of Lummerzheim and Lilensten.

[45] Figure 2 illustrates the daytime plus aurora (Figure 2a) and nighttime aurora (Figure 2b) model electron spectra used in this study, for altitudes of 130, 200, 280 and 350 km. The purpose of Figures 2a and 2b is to show the large differences in the low-energy portions of the electron distributions for the (relatively) electron-rich (Figure 2a) and electron-poor (Figure 2b) environments. Also shown in Figure 2 are the model electron spectra at 130 km (Figure 2c) and 350 km (Figure 2d), both for an IBC III^+ aurora, depicting the daytime plus aurora, nighttime aurora, daytime and nighttime thermal electron distributions. Note that the thermal distribution in all cases is that for the electron density and temperature from the IRI, without the subsequent changes predicted due to the aurora. The purpose of Figures 2c and 2d is to illustrate how each electron distribution differs at the lowest and highest altitudes used in this study. Ignoring the effect of the thermal electrons, Figure 2 shows that the electron spectrum at 350 km has a relatively greater abundance of high-energy electrons while that at 130 km has a greater abundance of "low"-energy (2–10 eV) electrons, as anticipated [see, e.g., *Lummerzheim and Lilensten*, 1994].

[46] As expected, the predicted vibrational distributions of N_2 are sensitive to both the detailed shape of the electron spectrum and to the strength of the aurora. Because a goal in this study was to determine the vibrational population distribution in N_2 as a function of altitude, care was taken to determine electron spectra which are representative at each altitude for a characteristic energy of 3.1 keV at the top of the atmosphere. In these calculations, the model electron spectrum at any altitude for an IBC Class III^+ aurora was obtained simply by multiplying the appropriate electron spectra for the IBC Class II^+ aurora by a factor of 10.

[47] The aurora causes an increase in the density of ions and balancing thermal electrons. The electron density calculated from the auroral flux is much smaller than required, thus there must be a low-energy tail of the secondary electron spectrum which is not available from the models or measurements described above. Also, as the electron temperature is dependent on excitation and deexcitation of molecular nitrogen, it needs to be determined as part of the detailed calculation. The temperature of the thermal electrons is calculated here by assuming that the energy flow rate into the thermal electrons is a fixed fraction of the ionization energy rate and that it is equal to the sum of the various electron cooling rates. These include the energy input rate (for excitation less deexcitation) from the thermal electrons into the vibrational levels of nitrogen, excitation of $O(^1D)$ and $O(^1S)$ (using cross sections of *Majeed and Strickland* [1997]), ion cooling [*Schunk and Nagy*, 1978], and excitation of the fine structure levels of O atoms (using collision strengths of *Bell et al.* [1998] and *Berrington* [1988], converted to cross sections as explained by *Pavlov and Berrington* [1999]). The thermal electron temperature is calculated by finding the value that makes these rates equal. The fraction of the energy input rate into the thermal electrons, relative to the ionization energy rate, was determined by adjusting the fraction until the calculated temperature was equal to that given in a previous work [*Vallance Jones*, 1974]. It was found that a fraction of 0.45 led to a calculated thermal electron temperature of ~3500 K at 300 km about 1 min after the onset of an IBC III^+ aurora, matching the value determined by Rees and Walker. [*Vallance Jones*, 1974]. The electron temperature

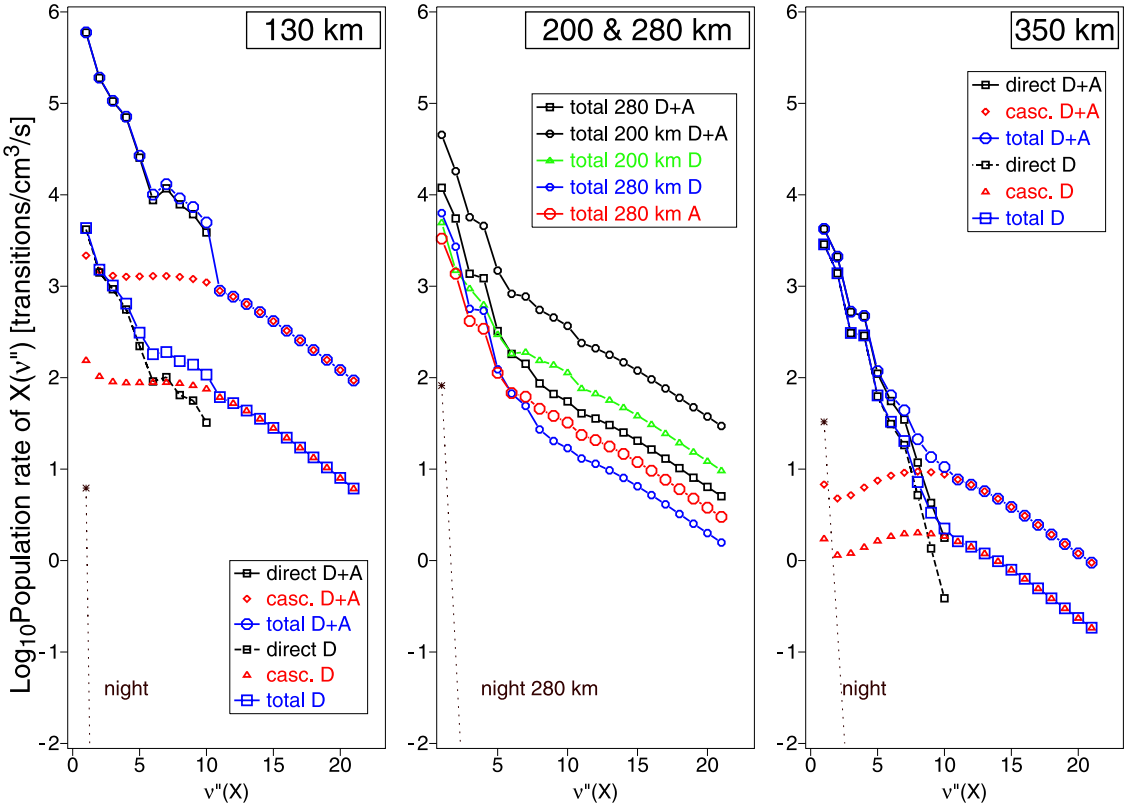

Figure 5. (left) Absolute direct, radiative cascade, and total population rates, as a function of vibrational quantum number, for daytime only and daytime plus an IBC II^+ aurora, all at 130 km. Shown are the individual contributions by direct and cascade mechanisms and the total rate. For comparison, the thermal population rate for night at 130 km is shown in the lower left. (middle) Same as Figure 5 (left) except for 200 and 280 km and that only the total population rates are shown. (right) Same as Figure 5 (left) except for an altitude of 350 km.

for the aurora in daytime is calculated to equate the energy rates as specified above, but with the nonauroral input added (As the daytime electron temperature is taken from the IRI model, the nonauroral energy input rate into N_2^* can be determined directly.). At higher altitudes most of excess energy from ionization events will be transported downward by secondary electrons, so the temperature was not recalculated at altitudes above 350 km.

[48] The electron densities and temperatures calculated for four different environments (IBC II^+ and IBC III^+ at night, and daytime plus IBC III^+) at the conclusion of the time step calculation are shown in Figure 3. The daytime density is consistent with the IRI, but the density is somewhat less (~15%) in the region of peak density. This difference might be due to an overestimation of the effect of N_2^* (to be discussed later), but may also be due to the cumulative effects in the calculation of inconsistencies between the atmospheric densities and temperatures determined from the MSIS and IRI models, respectively.

[49] The predicted temperature for the IBC III^+ nighttime aurora is slightly lower at 300 km than the value of 3500 K of Rees and Walker that was used in calibration. This is because, after 6 min, the electrons produced earlier have been cooled by excitation of N_2 so that "new" electrons being produced are being mixed with cooler electrons.

[50] The comparison for an IBC II^+ and IBC III^+ at night in Figure 3 shows that the electron temperature increases with auroral strength. As the auroral strength is scaled by multiplying the secondary electron spectrum by a constant, the energy input rate into the thermal electrons is scaled by the same factor and so the temperature might be expected to be independent of auroral strength. However, as the population of N_2^* builds up, the rate of electron cooling is reduced and the rate of deexcitation is increased. Thus the higher electron temperature for the IBC III^+ aurora is an indicator of the role of N_2^*.

4. Production of Vibrationally Excited N_2 in the Thermosphere

4.1. Relative Importance of Direct and Indirect Production of N_2^*

[51] Figure 4 shows our predicted fractional contributions to the total vibrational population of N_2 by (1) direct excitation and (2) radiative cascade from the $A^3\Sigma_u^+$ state and non-Rydberg singlet states, for altitudes of 130, 200 and 350 km and for daytime and aurora IBC II^+ conditions. Figure 4 illustrates the following general characteristics:

[52] 1. Except for aurora at 130 km, radiative cascade population of the $N_2[X]$ state is predicted to be >10% for $v'' > 4$, >20% for $v'' > 5$, and >50% for $v'' > 9$. Collisional

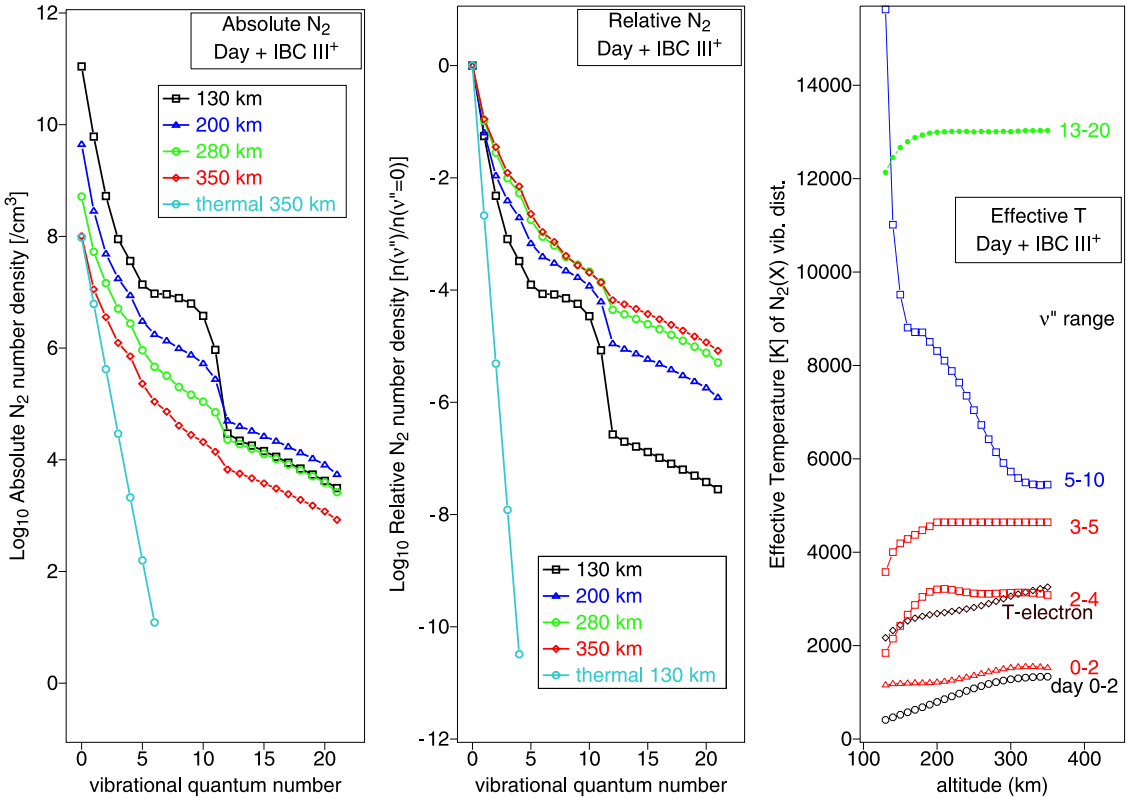

Figure 6. (left) Predicted absolute density of $N_2[X(\nu'')]$, as a function of the vibrational quantum number (ν'') and four different altitudes, for the daytime plus a 6-min aurora (IBC III$^+$). For purposes of comparison, the Boltzmann population at 350 km is also shown. (middle) Relative vibrational distributions (to that at $\nu'' = 0$) for each of the four altitudes, as a function of the vibrational quantum number. For purposes of comparison, the Boltzmann population of N_2 appropriate for an altitude of 130 km is also shown. (right) Electron temperature and the effective vibrational temperatures of the N_2 vibrational distribution as a function of altitude and for selected ranges of vibrational levels of the X state. The 0–2 vibrational temperature for daytime only is also shown ("day 0–2").

deactivation of the excited states is responsible for 130 km being different from the other altitudes.

[53] 2. Radiative cascade population from higher electronic states is responsible for 100% of the X state population for levels >10 because the direct excitation cross sections are effectively zero.

[54] 3. In the daytime, cascade population from the A state is comparable to that from the a state (see Figure 1) for $\nu'' < 5$ but is substantially greater for $\nu'' > 7$.

[55] 4. In the aurora, cascade population from the A state is greater than that from the a state for levels $\nu'' > 4$, except at 130 km where the transition takes place at $\nu'' = 10$.

4.2. Vibrational Populations, Effective Vibrational Temperatures, and Quanta

[56] Figure 5 shows the predicted [direct, radiative cascade, and total] absolute population rates by electron impact of the vibrational levels of N_2, as a function of the vibrational quantum number, for four selected altitudes. Figure 5 (left) shows the direct and cascade excitation rates separately for daytime and daytime plus aurora (IBC II$^+$) at an altitude of 130 km. Figure 5 (right) the same detail at 350 km. Figure 5 (middle) shows only the total population rates at 200 and 280 km for the daytime and daytime plus aurora (IBC II$^+$). The purpose of Figure 5 is to show clearly both the magnitude of the vibrational distribution and the relative contributions by direct and cascade population mechanisms, as a function of both the altitude and the electron environment. Note that the decreasing N_2 number density with altitude has been incorporated.

[57] Figures 6 and 7 provide detail as to the character of the predicted vibrational distributions produced by electron impact. Figure 6 shows the predicted absolute and relative vibrational distributions, and "effective" vibrational temperatures, for N_2 excited in an environment characterized by the daytime plus a 6-min IBC III$^+$ aurora, for altitudes of 130, 200, 280, and 350 km. Figure 7 shows the same quantities for a 6-min IBC III$^+$ strength aurora at night. Figures 6 (left) and 7 (left) show the predicted absolute number densities, and for comparison purposes, the Boltzmann distribution at 350 km is also shown. Figures 6 (middle) and 7 (middle) show the relative number densities for the same data as shown in Figures 6 (left) and 7 (left) and, again for comparison purposes, the relative Boltzmann population associated with 130 km. The drop in population at $\nu'' = 11$ at 130 km is due to the absence of excitation cross sections for $\nu'' > 10$ and the further drop at $\nu'' = 12$ is due to the reaction $N_2[X^1\Sigma_g^+ (\nu'' > 11)] + O \rightarrow NO + N$.

[58] From inspection of Figures 6 (middle) and 7 (middle), one can recognize the following qualitative characteristics

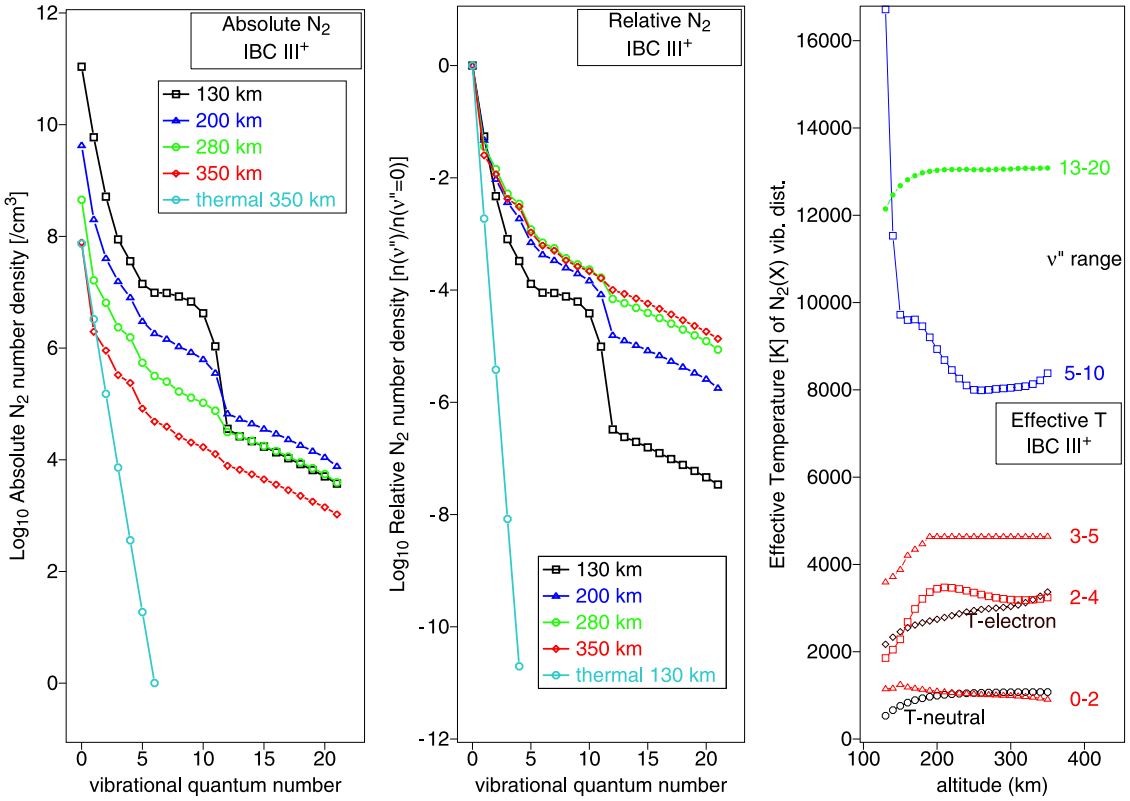

Figure 7. (left) Predicted absolute density of $N_2[X(\nu'')]$, as a function of the vibrational quantum number (ν'') and four different altitudes, for a 6-min aurora (IBC III$^+$) at night. For purposes of comparison, the Boltzmann population at 350 km is also shown. (middle) Relative vibrational distributions (to that at $\nu'' = 0$) for each of the four altitudes, as a function of the vibrational quantum number. For purposes of comparison, the Boltzmann population of N_2 appropriate for an altitude of 130 km is also shown. (right) Electron temperature and the effective vibrational temperatures of the N_2 vibrational distribution as a function of altitude and for selected ranges of vibrational levels of the X state. For comparison the IRI neutral temperature for nighttime without an aurora is also shown ("T neutral").

of the vibrational distributions predicted by our model: (1) because the relative populations for $\nu'' = 1$ and 2 in daytime plus IBC III$^+$ aurora increase with altitude, the "effective" vibrational temperature for levels $\nu'' = 0$, 1 and 2 increases with increasing altitude, and (2) the "effective" vibrational temperature for levels $\nu'' > 4$ is greater than that for levels $\nu'' \leq 4$ and approximately the same at all altitudes for levels $\nu'' > 11$, with and without the aurora.

[59] These qualitative conclusions are made quantitative in Figures 6 (right) and 7 (right), for their respective environments, in which the "effective" vibrational temperatures, as extracted from the vibrational distribution curves, are plotted as a function of altitude. In Figures 6 and 7, the calculated electron temperature is shown by diamonds.

[60] For levels 0–2, the vibrational temperatures for the daytime without aurora are also plotted in Figure 6. These are almost constant above 300 km due to molecular diffusion. In the aurora-only case, the vibrational temperature of the 0–2 levels is enhanced at lower altitudes, but decreases with height above 150 km, because, at the lower atmospheric densities, N_2^* does not reach an equilibrium during the limited duration of the aurora. Above 200 km the 0–2 curve for daytime plus aurora can be seen to be similar to the sum of the auroral temperatures with the daytime-only curve.

[61] For levels 2–4 the vibrational temperatures are seen to exceed the electron temperature. This can occur because they are being excited by higher-energy electrons in the secondary electron spectrum which have a higher effective temperature than the thermal electrons.

[62] The general conclusions from the results shown in Figures 6 and 7 are that the predicted vibrational distributions extend to higher vibrational levels than previously included in calculations and that the vibrational temperatures for levels above $\nu'' = 4$ have higher "effective" temperatures than the vibrational temperature determined by considering all the levels.

[63] The following key characteristics of the vibrational distributions predicted by our model and illustrated in Figures 6 and 7 are worth summarizing at this point.

[64] 1. At all altitudes, the "effective" temperature for levels >11 is essentially the same, for any environment, with a value between 12,000 and 13,000 K depending on the altitude. This is a direct result of the fact that these levels are populated by cascade from the A state so that the relative shape of the vibrational distribution for these levels will always be about the same, because the appropriate Franck-Condon factors connecting the A and X states are independent of the details of the electron source. The magnitude of the vibrational distribution will, of course, depend on the

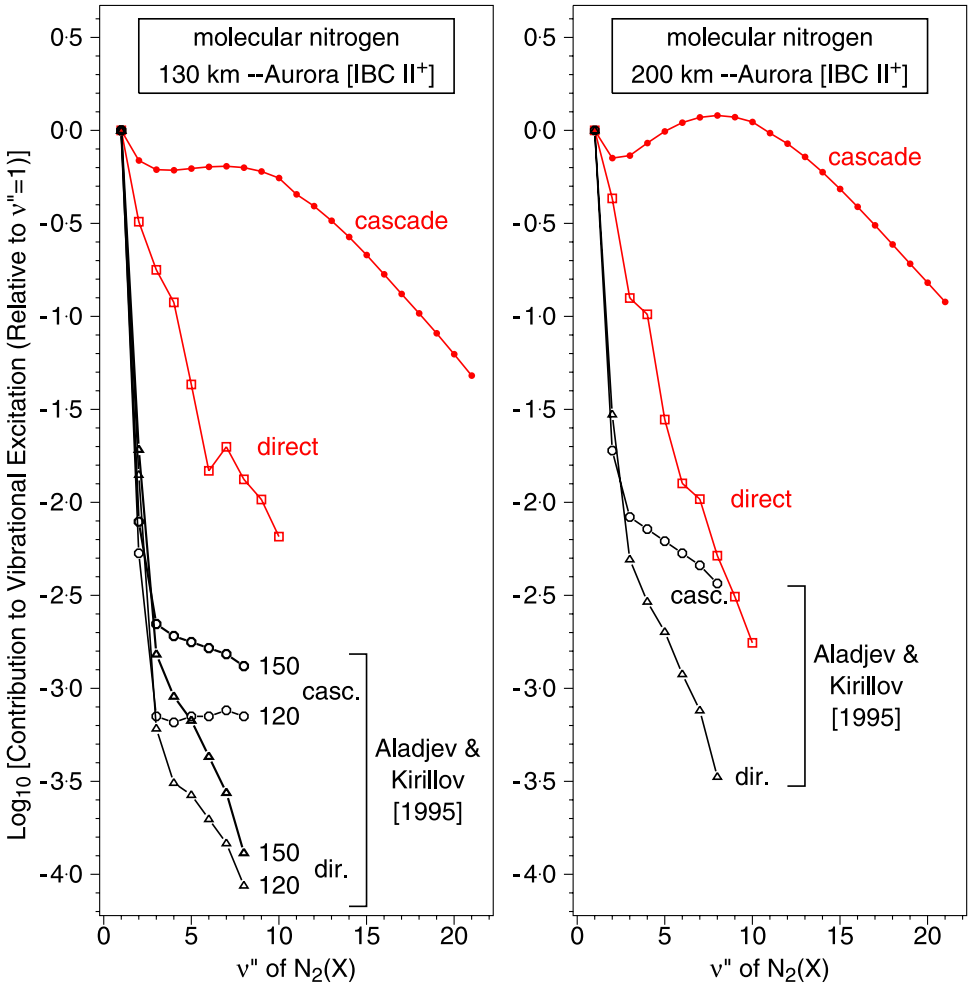

Figure 8. Relative (to $\nu'' = 1$) vibrational population (direct excitation and cascade excitation) rates to the N_2 ground state produced by an IBC II^+ aurora at (left) 130 km and (right) 200 km. The present results are shown by direct excitation (curve with squares) and cascade excitation contribution (curve with circles). Also shown in Figure 8 (left) are the direct and cascade predictions for 120 and 150 km from *Aladjev and Kirillov* [1995] and in Figure 8 (right) for 200 km.

details of the electron source but not the "effective" temperature because that depends only on the shape of the electron spectrum.

[65] 2. The "effective" temperature for the intermediate region of vibrational levels, $\nu'' = 5–10$, is apparently sensitive to the details of the total secondary electron distribution and the time for which it is applied, as indicated by the variation in the associated effective temperature shown in Figures 6 (right) and 7 (right).

[66] 3. The "effective" vibrational temperature for levels $\nu'' > 4$ is predicted to be in the range 4000–13000 K, depending on the altitude and environment. This result is generally greater than previously estimated and has the consequences discussed below.

[67] 4. As will also be shown below, the important quantity for determining the enhancement of O^+ charge transfer with vibrationally excited N_2 is the magnitude of the vibrational population for levels $\nu'' > 2$ relative to that at $\nu'' = 0$ or 1. As Figures 6 (middle) and 7 (middle) show, this quantity increases with increasing altitude for any particular environment, which suggests that the charge transfer rate should increase with increasing altitude, as is also described later.

[68] We note that *Vlasov and Smirnova* [1995a] examined the deviation of the calculated vibrational distribution from a Boltzmann distribution with altitude and solar activity, for daytime at middle latitudes. They reached the conclusion that the deviation from a Boltzmann distribution for the N_2 vibrational levels decreased with increasing altitude. They attributed this decrease to decreasing production, and increasing diffusion, associated with increasing altitude. The same conclusion can be drawn for an auroral case, at night or in daytime, from Figures 6 and 7, which show that the deviation from a straight line decreases with altitude.

[69] *Schunk and Hays* [1971] predicted that the higher vibrational temperatures due to aurora lead to an increased rate for the reaction $O^+ + N_2 \rightarrow NO^+ + N$, and the results shown in our Figures 6 and 7 support this finding. In addition, *Richards et al.* [1986] predicted that enhanced vibrational excitation leads to a reduction in the cooling rate of thermal electrons and so to higher electron temperatures. Before discussing the consequences of an enhanced vibra-

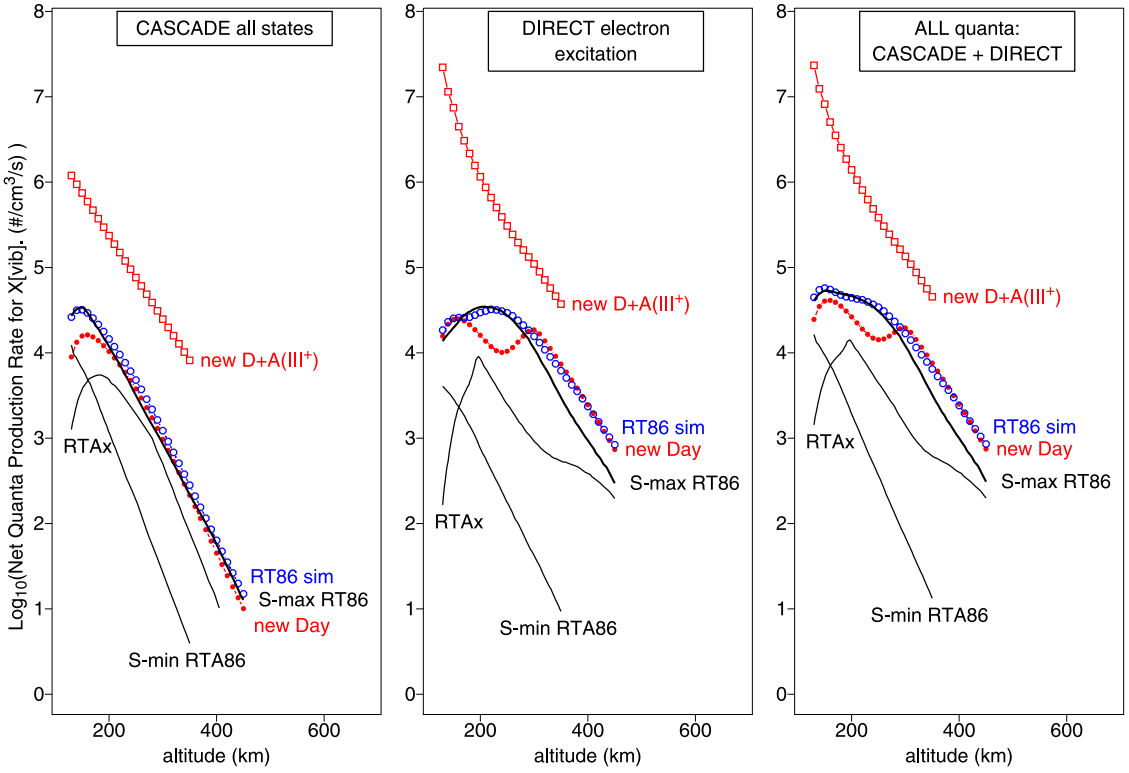

Figure 9. Net production rate of vibrational quanta, as a function of altitude, by (left) cascade from higher electronic states, (middle) direct electron excitation, and (right) the sum of both mechanisms, for daytime only (curve with solid circles) and for daytime plus an IBC III^+ aurora (curve with squares). Results for solar maximum (S max) conditions from *Richards and Torr* [1986] (RT86), and for solar minimum (S min) and solar maximum from *Richards et al.* [1986] (RTAx) are also shown, and the rates calculated for the conditions of *Richards and Torr* [1986] (RT86 sim) without N_2 excited state loss processes and using their calculated electron temperatures and O^+ densities (curve with open circles).

tional population, we first compare our predicted populations with comparable results previously reported for various mechanisms by which an enhanced vibrational population might be produced.

[70] Figure 8 compares the relative (to $\nu'' = 1$) contributions of direct and cascade population rates to the vibrational levels of the X state predicted by our model at altitudes of 130 and 200 km, as a function of the vibrational quantum number, with predictions from *Aladjev and Kirillov* [1995] for altitudes of 120, 150, and 200 km. In an effort to determine the conditions under which enhanced concentrations of NO might be formed in aurora, *Aladjev and Kirillov* [1995] examined the relative importance of collisions of $O(^1D)$ with N_2 and O_2 and kinetic-to-vibration [TV], elastic vibration-to-vibration [VV], and vibrational excitation/deexcitation [VV′] energy transfer processes among the atmospheric species, in addition to electron impact processes. However, for their electron impact spectrum they used a Maxwellian distribution, rather than a detailed auroral spectrum which has substantial flux at higher energies. This reduces, relative to the present results, the contribution to higher vibrational levels, and particularly to the excited states. As expected, their results are quantitatively different to ours (see Figure 8), but nevertheless, *Aladjev and Kirillov* [1995] reached the same conclusion as *Richards et al.* [1986] and this study in that cascade from the A state is the most probable mechanism for populating high vibrational levels of the X state.

[71] Figure 9 shows the predicted absolute net production rate of vibrational quanta, as a function of altitude, produced by direct, cascade, and total excitation for daytime and daytime plus auroral (IBC III^+) environments. The purpose of Figure 9 is to compare our predictions with those by *Richards and Torr* [1986] and by *Richards et al.* [1986], who reported the production of vibrational quanta associated with solar minimum and maximum conditions. Our predictions for cascade production are very similar to those for the same conditions (noon and midsummer, although at a different latitude) [*Richards and Torr*, 1986], except at 130 km, suggesting that our model includes greater quenching rates, while our predictions for direct excitation are substantially lower in the altitude range 150–290 km. This appears to be because the electron densities calculated by Richards and Torr (not given, but assumed to be larger than their plotted O^+ densities) are higher than the IRI values. These explanations for the discrepancies are confirmed by applying our model, simulating their calculation by excluding $A^3\Sigma_u^+$ collisional and chemical loss processes and fixing the O^+ densities and electron temperatures given by Richards and Torr. The electron density is calculated as the sum of their given O^+ densities and the densities of the other positive ions which we calculate due to ionization. In

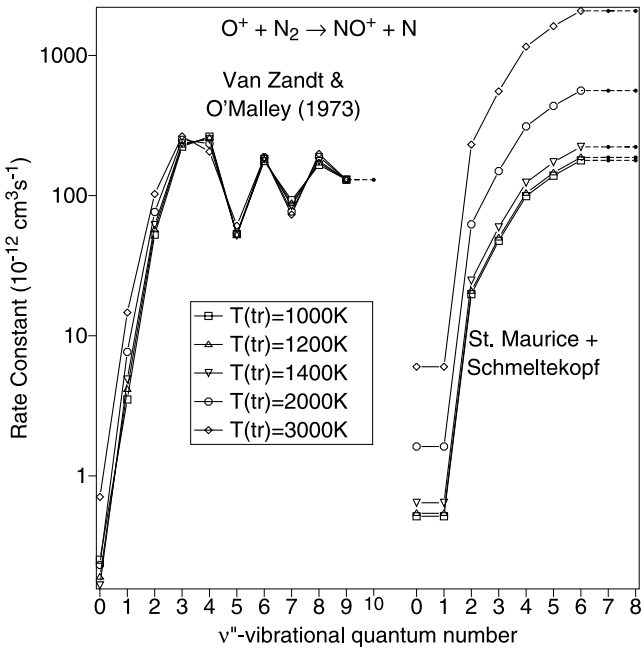

Figure 10. Rate constant [$cm^3\ s^{-1}$] for the $O^+ + N_2^* \rightarrow NO^+ + N$ charge exchange reaction, as a function of the vibrational quantum number and parametric on the translational temperature, extracted from the work of *Van Zandt and O'Malley* [1973] (left). For $\nu'' \geq 9$, an extrapolated constant value (dot-dashed) was assumed. The equivalent rate constants for the $\nu'' = 0$ value of *St.-Maurice and Torr* [1978] multiplied by the rate coefficients of *Schmeltekopf et al.* [1968] are shown on the right, with a similar indication of extrapolation for $\nu'' \geq 7$.

this case the agreement is very good up to 300 km. Overall, our predictions for daytime are in agreement with those from Richards and Torr, except for the calculated electron density. Hence the more elaborate model incorporated in this study substantiates the conclusions drawn by these previous studies.

[72] As would be expected, we predict a much greater production of quanta for an IBC III^+ aurora than for daytime. However, because of the higher electron density and temperature also produced by the aurora, the cascade contribution to production of vibrational quanta is quite small at all altitudes relative to direct electron excitation.

5. Role of Vibrationally Excited N_2 in the Thermosphere

5.1. Enhancement Factors for O^+ Charge Exchange

[73] The chemical reaction

$$(R1) \qquad O^+ + N_2 \rightarrow NO^+ + N$$

has been known to be important in determining the electron density in the ionosphere for many years, because diatomic molecular positive ions generally have electron recombination rates which are faster than those for atomic ions. The laboratory discovery [*Schmeltekopf et al.*, 1967, 1968] that the rate constant for reaction (R1) is strongly dependent on the degree of vibrational excitation of the N_2 molecule stimulated research on both the reaction itself and its consequences in the earth's ionosphere. The dependence of reaction (R1) on both the vibrational energy in N_2 and the relative kinetic energy of the O^+ and N_2 species has been studied experimentally [*Lindinger et al.*, 1974; *Albritton et al.*, 1977; *Hierl et al.*, 1997], from a theoretical collision physics perspective [*O'Malley*, 1970; *Van Zandt and O'Malley*, 1973], and for particularly nonthermal conditions in the thermosphere [*St.-Maurice and Torr*, 1978; *St.-Maurice and Laneville*, 1998]. In a simulation, *Newton et al.* [1974] found that deviations from the Boltzmann distribution for the N_2 vibrational population can produce an enhancement of reaction (R1) by a factor of 4 in the F_2 region. In their review of the formation of ionization troughs in the ionosphere, *Rodger et al.* [1992] characterized the general role of reaction (R1), and the analogous reaction with O_2, as the major electron loss processes in the F layer.

[74] We use the N_2 vibrational distributions described previously to estimate the enhancement of reaction (R1) due to the presence of our predicted vibrational distribution and its associated greater characteristic temperature than that of the local neutral temperature. A convenient way to characterize the enhancement of reaction (R1) is in terms of the "reaction rate enhancement factor", apparently first used by *Richards and Torr* [1986] and employed by many studies since then. This parameter is defined as

$$f = [k_0 n_0 + k_1 n_1 + k_2 n_2 + \ldots]/(k_0 n_0), \qquad (5)$$

where n_i is the density of vibrational level i and k_i is the associated rate constant for reaction (R1) for vibrational level i. The rate constants for reaction (R1) when the N_2 molecule is in vibrational level i, also a function of the translational (kinetic) temperature (T_{tr}) of the species in reaction (R1), were obtained directly from the work of *Van Zandt and O'Malley* [1973], as follows. Using the semiempirical model of *O'Malley* [1970], *Van Zandt and O'Malley* [1973] reported coefficients for the rate constant for reaction (R1), for vibrational levels 0 through 8, which reproduce the experimental results for $T_{tr} = 300$ K to 0.3% and all the experimental data available at that time to within 3% for $T_{tr} < 7000$ K. That rate constant is shown in Figure 10, as a function of the vibrational quantum number, for translational temperatures from 1000 to 3000 K. The first conclusion to be drawn from Figure 10 is that the rate constant for reaction (R1) is a weak function of the translational temperature relative to that demonstrated for the dependence on the first four N_2 vibrational quantum numbers [ν'']. The second conclusion is that since the "reaction rate enhancement factor" is defined as the rate for reaction (R1) for excited vibrational levels [$\nu'' > 0$] relative to that rate for $\nu'' = 0$, and the rate constant increases by a factor of 1000 from $\nu'' = 0$ to $\nu'' = 4$, it is immediately obvious that any appreciable vibrational population in levels $\nu'' > 1$ will have a dramatically faster rate than that in $\nu'' = 0$.

[75] A second (fortuitous) characteristic of the rate constant for reaction (R1) shown in Figure 10 is that predicted values from *Van Zandt and O'Malley* [1973] demonstrate virtually identical "damped" oscillations for $\nu'' > 4$ for all translational energies in the range shown in Figure 10. This behavior suggests that a reasonably accurate rate constant

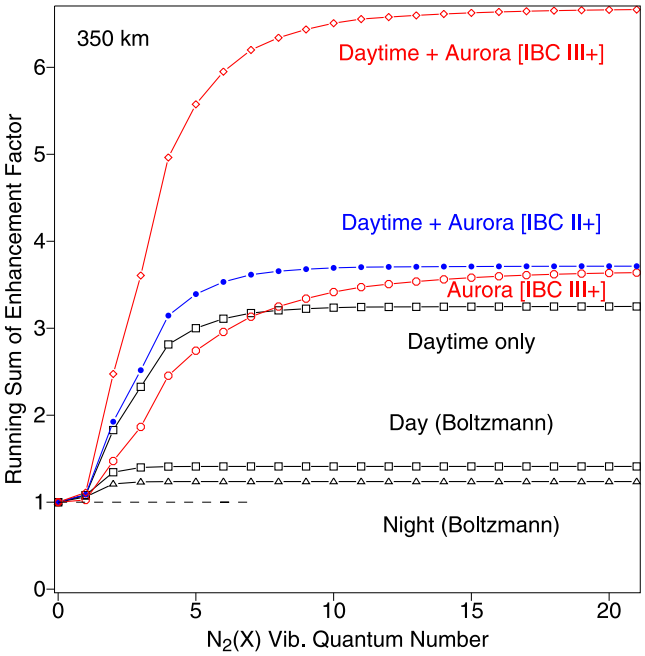

Figure 11. An example of the running sum of the predicted enhancement factor, as a function of the N_2 X state vibrational quantum number, for the daytime, an IBC III^+ nighttime aurora, and for the daytime and aurora (IBC II^+ and IBC III^+) together, all for the altitude of 350 km.

for $\nu'' = 8-21$ is represented by the average value of the rate constants for $\nu'' = 7$ and $\nu'' = 8$. That extrapolation, for $T_{tr} = 1200$ K, is shown in Figure 10 by dots. For the results reported here, a rate constant of 1.2978×10^{-10} cm^3 s^{-1} for levels $\nu'' = 9-21$, corresponding to a translational temperature of 1200 K, was used. For completeness, it is noted that the rate constant values for ν'' in the 8–21 range obtained by the above extrapolation method for different T_{tr} values in the range 1000–2000 K vary by less than 3% from a rate constant of 1.2978×10^{-10} cm^3 s^{-1}.

[76] In calculating the midday electron density it was found that if the vibrational enhancement of reaction R1 was not included, the density is too high. However, including vibrational enhancement with the rate constants of Van Zandt and O'Malley resulted in a density much lower than the IRI at the peak. Therefore the higher k_0 rate of *St.-Maurice and Torr* [1978] and the lower values of the enhancement using the rate coefficients of *Schmeltekopf et al.* [1968] were used. These rates are also plotted in Figure 10, where it can be seen that the difference between k_0 and the higher levels is considerably less, leading to a smaller enhancement factor. These smaller enhancement coefficients were used to calculate the electron density shown in Figure 3, which is still a little below the IRI at the peak, but closer than found using the rate constants of Van Zandt and O'Malley. Thus the rate constant of St. Maurice and Torr, combined with the rate coefficients of Smeltekopf et al., have been used for all calculations presented here. This is consistent with a conclusion of *Pavlov* [1998a].

5.2. Enhancement Factors in the Atmosphere

[77] Using the constants shown on the right of Figure 10 for the dependence of the rate constant for reaction (R1) on the vibrational quantum number, and the predicted vibrational distributions shown in Figures 6 and 7, the running sum defined by the quantity

$$S_r(\nu'') = \sum_{j=0}^{\nu''} k_j n_j / k_0 n_0 \qquad (6)$$

is shown in Figure 11, as a function of the vibrational quantum number ν''. The reason for showing the results obtained by using equation (6) is that those vibrational levels in N_2 which have the greatest effect on the rate enhancement factor for reaction (R1) can be clearly seen from Figure 11. That is, Figure 11 shows that the population in vibrational levels $\nu'' = 1-10$ determines the reaction rate enhancement factor defined in equation (5) and, as might be guessed based on the quantum number dependence of the reaction rate for (R1) shown in Figure 10, the greatest effect comes from the first 4 excited vibrational levels. Our model predicts that the enhancement factor increases with the increased "effective" temperature produced by the more energetic electron environments. As the cascade contribution from the excited states, relative to direct excitation, is significant only at levels above 4 (see Figure 4), Figure 11 also shows that the cascade contribution to the enhancement factor is small compared to direct excitation.

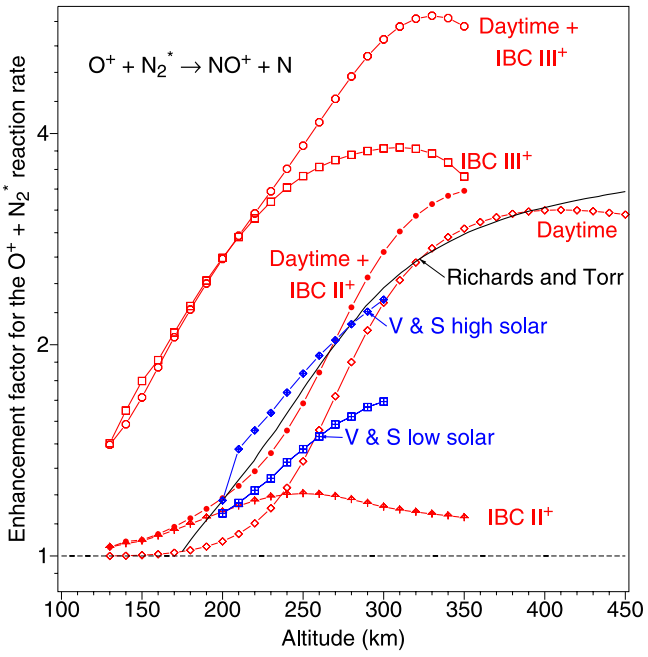

Figure 12. Predicted enhancement factor of the O^+ charge exchange reaction with N_2^* as a function of altitude, for normal daytime, and for 6-min IBC II^+ and III^+ aurorae, at night and in daytime. Shown for comparison are enhancement factors predicted for low and high solar activity (V & S) [*Vlasov and Smirnova*, 1995b] and for solar maximum [*Richards and Torr*, 1986].

[78] The enhancement factor of N_2^* is plotted in Figure 12, as a function of the altitude and for different environments. The following conclusions can be drawn from the results shown in Figure 12. The electron excitation mechanism for producing vibrationally excited N_2, predicts that the associated rate enhancement factor for reaction (R1) (1) increases with altitude for any of the electron environments up to a maximum and then declines, with a maximum at a height that increases with auroral strength, (2) increases with auroral strength, and (3) increases with auroral strength in daytime. These results follow directly from the electron impact model used here in that any increase in the number and/or average energy of the electrons is predicted to result in an increased population of the higher [i.e., $\nu'' > 1$] vibrational levels of N_2 and hence an enhancement in reaction (R1).

[79] Also shown in Figure 12 are enhancement factors calculated by other authors. The enhancement factor of *Richards and Torr* [1986] is determined using the same enhancement coefficients as used in this work. At lower altitudes the current predictions for daytime are lower than those of Richards and Torr but agree at higher altitudes. The predicted enhancement factors for an anharmonic oscillator model of nitrogen, for both high and low solar activity, are similarly higher than the current values at low altitiudes. The discrepancy may arise from the use here of more recent photoionization models, VV rates, chemical reaction rates and electron cross sections.

6. Conclusions

[80] A statistical equilibrium model for calculating the excited state and ground electronic state vibrational populations of molecular nitrogen produced by electron impact has been improved by incorporating the most recent electron impact excitation cross sections for molecular nitrogen. This model has also been extended to include VT and VV thermal interactions and a model of atmospheric processes in order to take account of chemical reactions involved in the production and loss of vibrationally excited nitrogen. Molecular and ambipolar diffusion is also included. A detailed auroral electron spectrum has been assembled from various models and measurements and a method to calculate the increase in the thermal electron temperature during auroral excitation has been implemented.

[81] A time step version of the statistical equilibrium model was also developed in this study to allow the calculation to be performed in circumstances where the atmospheric constituents do not reach equilibrium, such as in a limited duration aurora and below the altitudes where diffusion dominates.

[82] Results from our study show that in the ionosphere and polar thermosphere:

[83] 1. Direct electron impact excitation from $N_2[X(\nu'' = 0)]$, plus chemical reactions and thermal transitions, largely determines the population of the lowest few (i.e., $\nu'' < 5$) excited vibrational levels in the $N_2[X]$ state,

[84] 2. Electron impact excitation of higher N_2 electronic states, followed by cascade back down into the ground electronic state, largely determines the population of the higher (i.e., $\nu'' \geq 5$) vibrational levels,

[85] 3. The effective ground state vibrational temperature for levels greater than $\nu'' > 4$ in N_2 is predicted to be in the range 4000–13000 K for altitudes greater than 200 km.

[86] Calculations of relative population rates are compared with those of a previous study for an auroral environment that used a Maxwellian distribution for the electron spectrum. The current study gives very different results, with much higher contributions at higher vibrational levels for both the ground and excited states, presumably due to the use here of a detailed auroral electron spectrum, which has significant flux at higher electron energies where the Maxwellian distribution is negligible.

[87] In contrast, a comparison with a previous study of the net production of vibrational quanta in daytime shows substantial agreement, particularly when the input parameters of our model are set to match the previous study as closely as possible. This highlights the importance of using a detailed electron spectrum rather than a Maxwellian distribution. It also suggests that in the calculation of vibrational quanta the inclusion of detailed cascade calculations and new electron impact cross sections has only made a small difference to the overall result.

[88] The ability to reproduce previous results for daytime with the present model appears to be inconsistent with the extended vibrational population and higher vibrational temperatures predicted by the current model. However, production rates of vibrational quanta are not particularly sensitive to the higher levels as the excitation rate is weighted by just the quantum number. The reaction rate with vibrationally excited N_2 with O^+ is much more sensitive to the population of the higher levels because the reaction rate for these is much greater than for levels 0 or 1.

[89] The implication of the extended vibrational population for the reaction rate between O^+ and vibrationally excited N_2 was investigated, by calculation of a previously defined enhancement factor. The increases for the atmosphere found in this study are similar to ratios reported in previous work, but substantially smaller at lower altitudes for normal daytime. It was found that the enhancement of the reaction increases with both altitude and auroral activity, up to a maximum at a height which increases with auroral strength.

[90] Although the detailed calculation of the cascade between and from excited states into the vibrational levels of the ground state of N_2 produces an extended vibrational population compared to previous calculations, it does not make a significant difference in the estimates of the production of vibrational quanta or of the enhancement factor in the aurora, as both of these are dominated by ground state levels $\nu'' < 5$, to which the cascade contribution is relatively small.

[91] The production or loss of nitric oxide is involved in several of the reactions involving vibrationally excited nitrogen. As previously noted in our introduction, application of the current model to the prediction of nitric oxide density will be addressed by L. Campbell et al. (manuscript in preparation, 2006).

[92] **Acknowledgments.** This work was supported by the Australian Research Council and Flinders University.

[93] Arthur Richmond thanks Michael Vlasov and P. Swaminathan for their assistance in evaluating this paper.

References

Aladjev, G. A., and A. S. Kirillov (1995), Vibrational kinetics of molecular nitrogen and its role in the composition of the polar thermosphere, *Adv. Space Res.*, *16*(l), 109–112.

Albritton, D. L., I. Dotan, W. Lindinger, M. McFarland, J. Tellinghuisen, and F. C. Fehsenfeld (1977), Effects of ion speed distributions in flow-drift tube studies of ion-neutral reactions, *J. Chem. Phys.*, *66*, 410–421.

Bailey, G. J., A. E. Ennis, and R. J. Moffett (1997), The effect of vibrationally excited nitrogen on the low-latitude Ionosphere, *Ann. Geophys.*, *15*, 1422–1428.

Barth, C. A. (1992), Nitric oxide in the lower thermosphere, *Planet. Space Sci.*, *40*, 315–336.

Bell, K. L., K. A. Berrington, and M. R. J. Thomas (1998), Electron impact excitation of the ground-state ^{3}P fine-structure levels in atomic oxygen, *Mon. Not. R. Astron. Soc.*, *293*, L83–L87.

Berrington, K. A. (1988), Low-energy electron excitation of the $^3P^e$ fine-structure levels in atomic oxygen, *J. Phys. B At. Mol. Opt. Phys.*, *21*, 1083–1089.

Bilitza, D. (2001), International Reference Ionosphere 2000, *Radio Sci.*, *36*, 261–275.

Breig, E. L., M. E. Brennen, and R. J. McNeal (1973), Effect of atomic oxygen upon the N_2 vibrational temperature in the lower thermosphere, *J. Geophys. Res.*, *78*, 1225–1228.

Broadfoot, A. L., D. B. Hatfield, E. R. Anderson, T. C. Stone, B. R. Sandel, J. A. Gardner, E. Murad, D. J. Knecht, and C. P. Pike (1997), N_2 triplet band systems and atomic oxygen in the dayglow, *J. Geophys. Res.*, *102*, 11,567–11,584.

Brunger, M. J., and S. J. Buckman (2002), Electron-molecule scattering cross-sections. I. Experimental techniques and data for diatomic molecules, *Phys. Rep.*, *357*, 215–458.

Brunger, M. J., S. J. Buckman, and M. T. Elford (2003), Integral cross sections for electron impact excitation of molecules, in *Electron Collisions With Molecules: Scattering and Excitation*, Landolt-Börnstein vol. I/17C, edited by Y. Itikawa, pp. 6-132 to 6-145, chap. 6.4, Springer, New York.

Buonsanto, M. J., D. P. Sipler, G. B. Davenport, and J. M. Holt (1997), Estimation of the O^+, O collision frequency from coincident radar and Fabry-Perot observations at Millstone Hill, *J. Geophys. Res.*, *102*, 17,267–17,274.

Campbell, L., M. J. Brunger, A. M. Nolan, L. J. Kelly, A. B. Wedding, J. Harrison, P. J. O. Teubner, D. C. Cartwright, and B. McLaughlin (2001), Integral cross sections for electron impact excitation of electronic states of N_2, *J. Phys. B At. Mol. Opt. Phys.*, *34*, 1185–1199.

Campbell, L., M. J. Brunger, D. C. Cartwright, and P. J. O. Teubner (2004), Production of vibrationally excited N_2 by electron impact, *Planet. Space Sci.*, *52*, 815–822.

Cartwright, D. C. (1978), Vibrational populations of the excited states of N_2 under auroral conditions, *J. Geophys. Res.*, *83*, 517–531.

Cartwright, D. C., M. J. Brunger, L. Campbell, B. Mojarrabi, and P. J. O. Teubner (2000), Nitric oxide excited under auroral conditions: Excited state densities and band emissions, *J. Geophys. Res.*, *105*, 20,857–20,867.

Cosby, P. C. (1993), Electron-impact dissociation of nitrogen, *J. Chem. Phys.*, *98*, 9544–9553.

Eastes, R. W. (2000), Modeling the N_2 Lyman-Birge-Hopfield bands in the dayglow: Including radiative and collisional cascading between the singlet states, *J. Geophys. Res.*, *105*, 18,557–18,573.

Ennis, A. E., G. J. Bailey, and R. J. Moffett (1995), Vibrational nitrogen concentration in the ionosphere and its dependence on season and solar cycle, *Ann. Geophys.*, *13*, 1164–1171.

Feldman, P. D., and J. P. Doering (1975), Auroral electrons and the optical emissions of nitrogen, *J. Geophys. Res.*, *80*, 2808–2812.

Gilmore, F. R. (1965), Potential energy curves for N_2, NO, O_2 and corresponding ions, *J. Quant. Spectrosc. Radiat. Transfer*, *5*, 369–389.

Gilmore, F. R., R. R. Laher, and P. J. Espy (1992), Franck-Condon factors, r-centroids, electronic transition moments, and Einstein coefficients for many nitrogen and oxygen band systems, *J. Phys. Chem. Ref. Data*, *21*, 1005–1107.

Gordiyets, V. F. (1977), Vibrational relaxation of anharmonic N_2 molecules and concentration of nitrogen oxide in a disturbed thermosphere, *Geomagn. Aeron.*, *17*, 578–582.

Herron, J. T. (1999), Evaluated chemical kinetics data for reactions of $N(^2D)$, $N(^2P)$, and N_2 ($A^3\Sigma_u^+$) in the gas phase, *J. Phys. Chem. Ref. Data*, *28*, 1453–1483.

Hierl, P. M., I. Dotan, J. V. Seeley, J. M. Van Doren, R. A. Morris, and A. A. Viggiano (1997), Rate constants for the reactions of O^+ with N_2 and O_2 as a function of temperature (300–1800 K), *J. Chem. Phys.*, *106*, 3540–3544.

Itikawa, Y., and A. Ichimura (1990), Cross sections for collisions of electrons and photons with atomic Oxygen, *J. Phys. Chem. Ref. Data*, *19*, 637–651.

Jenkins, B., G. J. Bailey, A. E. Ennis, and R. J. Moffett (1997), The effect of vibrationally excited nitrogen on the low-altitude ionosphere, *Ann. Geophys.*, *15*, 1422–1428.

Kawashima, T., K.-I. Oyama, K. Suzuki, N. Iwagami, and S. Teii (1997), A measurement of the N_2 number density and the N_2 vibrational rotational temperature in the lower thermosphere—Instrumentation and preliminary results, *Adv. Space Res.*, *19*(4), 663–666.

Kochetov, I. V., E. V. Mishin, and V. A. Telegin (1987), Oxidation of nitrogen in nonequilibrium weakly ionized plasmas, *Sov. Phys. Dokl.*, Engl. Transl., *31*, 990–992.

Kolesnik, A. G. (1982), Vibrational temperature of nitrogen in the ionospheric *F* region (self-consistent calculation), *Geomagn. Aeron.*, *22*, 496–500.

Kirillov, A. S. (1998), The calculation of TV, VT, VV, VV′-rate coefficients for the collisions of the main atmospheric components, *Ann. Geophys.*, *16*, 838–846.

Kummler, R. H., and M. H. Bortner (1972), Vibrational temperatures in the *E* and *F* regions, in *COSPAR Space Research XII*, vol. 1, pp. 711–719, Akademie, Berlin.

Lindinger, W., F. C. Fehsenfeld, A. L. Schmeltekopf, and E. E. Ferguson (1974), Temperature dependence of some ionospheric ion-neutral reactions from 300°–900° K, *J. Geophys. Res.*, *79*, 4753–4756.

Lindsay, B. G., and M. A. Mangan (2003), Electron-impact ionization, in *Cross Sections for Ion Production by Electron Collisions With Molecules*, Landolt-Börnstein vol. I/17C, edited by Y. Itikawa, pp. 5-67 to 5-68, Springer, New York.

Lofthus, A., and P. H. Krupenie (1977), The spectrum of molecular nitrogen, *J. Phys. Chem. Ref. Data*, *6*, 113–307.

Lummerzheim, D., and J. Lilensten (1994), Electron transport and energy degradation in the ionosphere: Evaluation of the numerical solution, comparison with laboratory experiments and auroral observations, *Ann. Geophys.*, *12*, 1039–1051.

Lummerzheim, D., M. H. Rees, and H. R. Anderson (1989), Angular dependent transport of auroral electrons in the upper atmosphere, *Planet. Space Sci.*, *37*, 109–129.

Majeed, T., and D. J. Strickland (1997), New survey of electron impact cross sections for photoelectron and auroral electron energy loss calculations, *J. Phys. Chem. Ref. Data*, *26*, 335–349.

Mishin, Y. V., and V. A. Telegin (1989), Effects of plasma turbulence on auroras (A review), *Geomagn. Aeron.*, Engl. Transl., *29*, 1–12.

Moffett, R. J., A. E. Ennis, G. J. Bailey, R. A. Heelis, and L. H. Brace (1998), Electron temperatures during rapid subauroral ion drift events, *Ann. Geophys.*, *16*, 450–459.

Morrill, J. S., and W. M. Benesch (1996), Auroral N_2 emissions and the effect of collisional processes on N_2 triplet state vibrational populations, *J. Geophys. Res.*, *101*, 261–274.

Morrill, J. S., E. J. Bucsela, V. P. Pasko, S. L. Berg, M. J. Heavner, D. R. Moudry, W. M. Benesch, E. M. Wescott, and D. D. Sentman (1998), Time resolved N_2 triplet state vibrational populations and emissions associated with red sprites, *J. Atmos. Sol. Terr. Phys.*, *60*, 811–829.

Newton, G. P., J. C. G. Walker, and P. H. E. Meijer (1974), Vibrationally excited nitrogen in stable auroral red arcs and its effect on ionospheric recombination, *J. Geophys. Res.*, *79*, 3807–3818.

O'Malley, T. F. (1970), Simple model for the high energy reaction of O^+ ions with N_2^*, *J. Chem. Phys.*, *52*, 3269–3277.

O'Neil, R. R., W. R. Pendleton Jr., A. M. Hart, and A. T. Stair Jr. (1974), Vibrational temperature and molecular density of thermospheric nitrogen measured by rocket-borne electron beam induced luminescence, *J. Geophys. Res.*, *79*, 1942–1958.

Pavlov, A. V. (1993), The role of vibrationally excited nitrogen in the formation of the mid-latitude ionisation trough, *Ann. Geophys.*, *11*, 479–484.

Pavlov, A. V. (1998a), The role of vibrationally excited oxygen and nitrogen in the ionosphere during the undisturbed and geomagnetic storm period of 6–12 April 1990, *Ann. Geophys.*, *16*, 589–601.

Pavlov, A. V. (1998b), New electron energy transfer rates for vibrational excitation of N_2, *Ann. Geophys.*, *16*, 176–182.

Pavlov, A. V., and K. A. Berrington (1999), Cooling rate of thermal electrons by electron impact excitation of fine structure levels of atomic oxygen, *Ann. Geophys.*, *17*, 919–924.

Pavlov, A. V., and M. J. Buonsanto (1996), Using steady state vibrational temperatures to model effects of N_2* on calculations of electron densities, *J. Geophys. Res.*, *101*, 26,941–26,945.

Pavlov, A. V., and M. J. Buonsanto (1998), Anomalous electron density events in the quiet summer ionosphere at solar minimum over Millstone Hill, *Ann. Geophys.*, *16*, 460–469.

Pavlov, A. V., and A. A. Namgaladze (1988), Vibrationally-excited molecular nitrogen in the upper atmosphere (review), *Geomagn. Aeron.*, *28*, 607–620.

Pavlov, A. V., and K.-I. Oyama (2000), The role of vibrationally excited nitrogen and oxygen in the ionosphere over Millstone Hill during 16–23 March, 1990, *Ann. Geophys.*, *18*, 957–966.

Pavlov, A. V., T. Abe, and K.-I. Oyama (2000), Comparison of the measured and modelled electron densities and temperatures in the ionosphere and plasmasphere during 20–30 January, 1993, *Ann. Geophys.*, *18*, 1257–1272.

Reidy, W. P., T. C. Degges, A. G. Hurd, A. T. Stair Jr., and J. C. Ulwick (1982), Auroral nitric oxide concentration and infrared emission, *J. Geophys. Res.*, *87*, 3591–3598.

Richards, P. G., and D. G. Torr (1986), A factor of 2 reduction in theoretical F2 peak electron density due to enhanced vibrational excitation of N_2 in summer at solar maximum, *J. Geophys. Res.*, *91*, 11,331–11,336.

Richards, P. G., D. G. Torr, and W. A. Abdou (1986), Effects of vibrational enhancement of N_2 on the cooling rate of ionospheric thermal electrons, *J. Geophys. Res.*, *91*, 304–310.

Richards, P. G., J. A. Fennelly, and D. G. Torr (1994), EUVAC: A solar EUV flux model for aeronomic calculations, *J. Geophys. Res.*, *99*, 8981–8992.

Rodger, A. S., R. J. Moffett, and S. Quegan (1992), The role of ion drift in the formation of ionisation troughs in the mid- and high-latitude ionosphere—A review, *J. Atmos. Terr. Phys.*, *54*, 1–30.

Rusanov, V. D., A. A. Fridman, and G. V. Sholin (1981), The physics of a chemically active plasma with nonequilibrium vibrational excitation of molecules, *Sov. Phys. Usp.*, Engl. Transl., *24*, 447–474.

Schmeltekopf, A. L., F. C. Fehsenfeld, G. I. Gilman, and E. E. Ferguson (1967), Reaction of atomic oxygen ions with vibrationally excited nitrogen molecules, *Planet. Space Sci.*, *15*, 401–406.

Schmeltekopf, A. L., E. E. Ferguson, and F. C. Fehsenfeld (1968), Afterglow studies of the reactions He^+, He (2^3S), and O^+ with vibrationally excited N_2, *J. Chem. Phys.*, *48*, 2966–2973.

Schulz, G. J. (1964), Vibrational excitation of N_2, CO and H_2 by electron impact, *Phys. Rev. A*, *135*, 988–994.

Schulz, G. J. (1976), A review of vibrational excitation of molecules by electron impact at low energies, in *Principles of Laser Plasmas*, edited by G. Berkefi, p. 33, Wiley-Interscience, Hoboken, N. J.

Schunk, R. W., and P. B. Hays (1971), Theoretical N_2 vibrational distribution in an aurora, *Planet. Space Sci.*, *19*, 1457–1461.

Schunk, R. W., and A. F. Nagy (1978), Electron temperatures in the *F* region of the ionosphere: Theory and observations, *Rev. Geophys.*, *16*, 355–399.

Sharp, W. E., and P. B. Hays (1974), Low-energy auroral electrons, *J. Geophys. Res.*, *79*, 4319–4321.

Solomon, S. C., S. M. Bailey, and T. N. Woods (2001), Effect of solar soft X-rays on the lower ionosphere, *Geophys. Res. Lett.*, *28*, 2149–2152.

St.-Maurice, J.-P., and P. J. Laneville (1998), Reaction of O^+ with O_2, N_2, and NO under highly disturbed auroral conditions, *J. Geophys. Res.*, *103*, 17,519–17,521.

St.-Maurice, J.-P., and D. G. Torr (1978), Nonthermal rate coefficients in the ionospere: The reactions of O^+ with N_2, O_2, and NO, *J. Geophys. Res.*, *83*, 969–977.

Strickland, D. J., J. Bishop, J. S. Evans, T. Majeed, P. M. Shen, R. J. Cox, R. Link, and R. E. Huffman (1999), Atmospheric Ultraviolet Radiance Integrated Code (AURIC): Theory, software architecture, inputs, and selected results, *J. Quant. Spectrosc. Radiat. Transfer*, *62*, 689–742.

Stubbe, P., and W. S. Varnum (1972), Electron energy transfer rates in the ionosphere, *Planet. Space Sci.*, *20*, 1121–1126.

Swaminathan, P. K., et al. (1998), Nitric oxide abundance in the mesosphere/lower thermosphere region: Roles of solar soft X rays, suprathermal N(^{4}S) atoms, and vertical transport, *J. Geophys. Res.*, *103*, 11,579–11,594.

Swider, W. (1976), Atmospheric formation of NO from $N_2(A^3\Sigma)$, *Geophys. Res. Lett.*, *3*, 335–337.

Torr, D. G., K. Donahue, D. W. Rusch, M. R. Torr, A. O. Nier, D. Kayser, W. B. Hanson, and J. H. Hoffman (1979), Charge exchange of metastable ^{2}D oxygen ions with molecular oxygen: A new source of thermospheric O_2^+ ions, *J. Geophys. Res.*, *84*, 387–392.

Torr, D. G., M. R. Torr, and P. G. Richards (1980), Causes of the F region winter anomaly, *Geophys. Res. Lett.*, *7*, 301–304.

Trajmar, S., D. F. Register, and A. Chutjian (1983), Electron scattering by molecules II. Experimental methods and data, *Phys. Rep.*, *97*, 219–356.

Vallance Jones, A. (1974), *Aurora*, p. 45 and appendix 3B, Springer, New York.

Van Zandt, T. E., and T. F. O'Malley (1973), Rate coefficient for the reaction of O^+ with vibrationally excited N_2, *J. Geophys. Res.*, *78*, 6818–6820.

Varnum, W. S. (1972), Enhanced N_2 vibrational temperatures in the thermosphere, *Planet. Space Sci.*, *20*, 1865–1873.

Vlasov, M. N. (1972), Vibrationally-excited nitrogen in the upper atmosphere, *Geomagn. Aeron.*, *12*, 422–425.

Vlaskov, V. A., and K. Henriksen (1985), Vibrational temperature and excess vibrational energy of molecular nitrogen in the ground state derived from N_2^+ emission bands in aurora, *Planet. Space Sci.*, *33*, 141–145.

Vlasov, M. N., and T. M. Izakova (1980), Role of vibrational excitation in the formation of the winter anomaly of the ionospheric plasma, *Dokl. Earth Sci. Sect.*, *254*, 1–4.

Vlasov, M. N., and M. C. Kelley (2003), Modeling of the electron density depletion in the storm-time trough on April 20, 1985, *J. Atmos. Solar Terr. Phys.*, *65*, 211–217.

Vlasov, M. N., and I. A. Smirnova (1995a), Vibrational kinetics of molecular nitrogen as anharmonic molecules in the thermosphere, *Cosmic Res.*, *33*, 72–78.

Vlasov, M. N., and I. A. Smirnova (1995b), Role of nitrogen molecules as anharmonic oscillators in ionospheric F2–region recombination, *Cosmic Res.*, *33*, 135–138.

Vlasov, M. N., and I. A. Smirnova (1997), Role of the vibrational excitation for the nitric oxide production in the polar thermosphere, *Cosmic Res.*, *35*, 321–324.

Vlasov, M. N., V. I. Chernyshev, and V. G. Kolesnik (1978), Distribution of molecular nitrogen by vibrational levels in the upper atmosphere, *Geomagn. Aeron.*, *18*, 440–443.

Vlasov, M. N., Y. V. Mishin, and V. A. Telegin (1980), Mechanism of formation of high nitric oxide concentrations in the polar ionosphere, *Geomagn. Aeron.*, Engl. Transl., *20*, 36–38.

Waite, J. H., A. F. Nagy, and D. G. Torr (1979), N2 vibrational distribution in aurorae, *Planet. Space Sci.*, *27*, 901–903.

Walker, J. C. G. (1968), Electron and nitrogen vibrational temperature in the *E*-region of the ionosphere, *Planet. Space Sci.*, *16*, 321–327.

Walker, J. C. G., R. S. Stolarski, and A. F. Nagy (1969), The vibrational temperature of molecular nitrogen in the thermosphere, *Ann. Geophys.*, *25*, 831–839.

Wiese, W. L., M. W. Smith, and B. M. Glennon (1996), *Atomic Transition Probabilities*, vol. I, *Hydrogen Through Neon*, *Natl. Stand. Ref. Data Ser.*, *NSRDS-NBS 4*, 55.

Zhdanok, S. A., and V. A. Telegin (1983), Dynamics for establishment of N_2 molecule distribution function by vibration levels and NO formation in polar auroral arcs, *Geomagn. Aeron.*, Engl. Transl., *23*, 266–267.

M. J. Brunger, L. Campbell, and P. J. O. Teubner, ARC Centre for Antimatter-Matter Studies, School of Chemistry, Physics and Earth Sciences, Flinders University, GPO Box 2100, Adelaide, SA 5001, Australia. (laurence.campbell@flinders.edu.au)

D. C. Cartwright, Theoretical Divisions, Los Alamos National Laboratory, Los Alamos, NM 87545, USA.